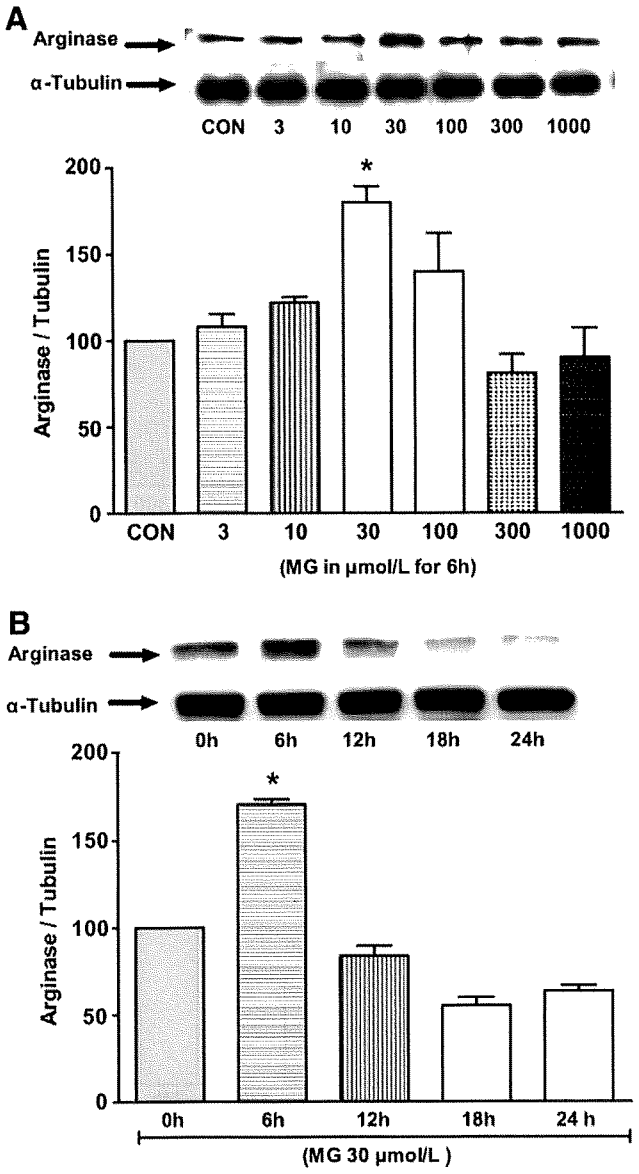

Figure 6. Effect of MG on endothelial arginase II expression. Representative Western blot shows increased arginase II expression normalized to α-tubulin in endothelial cells (A) treated with MG (0 to 1000 μmol/L) for 6 hours and (B) treated with 30 μmol/L of MG for 24 hours. Graphs shown are a summary of 5 independent experiments. *$P<0.05$.

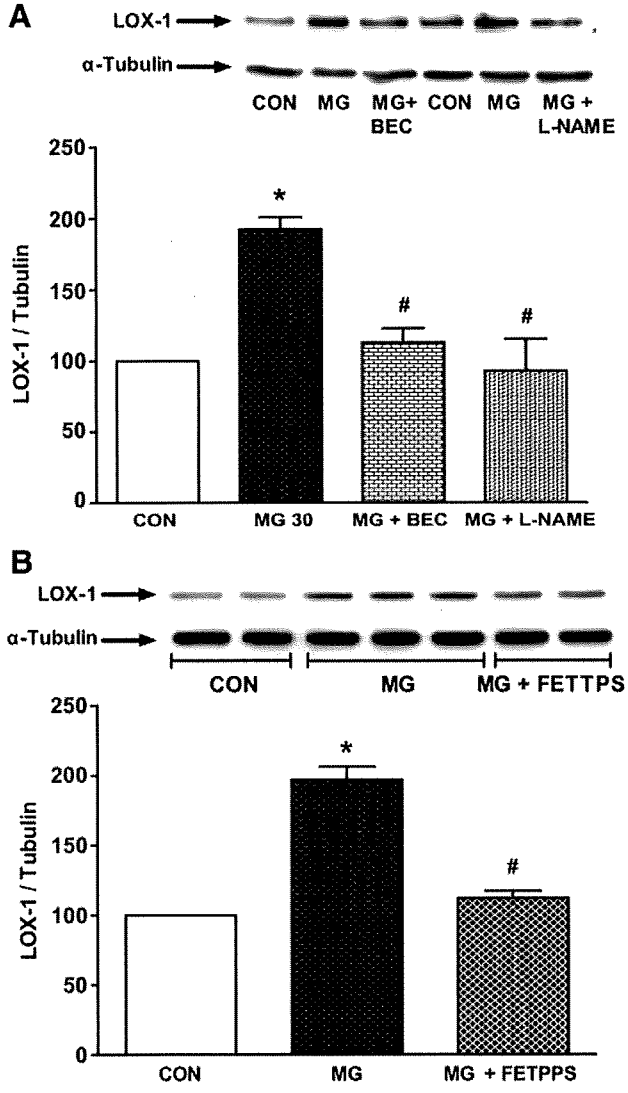

Figure 7. Effect of arginase and NOS inhibition on LOX-1 expression. Representative Western blot showing increased LOX-1 expression in response to MG (30 μmol/L) for 24 hours in the presence or absence of (A) BEC and L-NAME and (B) FeTPPS. Graph shows the summary of 5 independent experiments. *$P<0.05$ control (CON) vs MG; #$P<0.05$ MG vs MG+BEC, MG+L-NAME, or MG+FeTPPS.

NOS played a role in the upregulation of LOX-1 in response to MG. MG (30 μmol/L) treatment of endothelial cells for 24 hours upregulated LOX-1 expression by ≈100% ($P<0.05$), which was significantly reduced to control levels by arginase or NOS inhibition with BEC or L-NAME, respectively ($P<0.05$; Figure 7A). Because LOX-1 is involved in the binding and uptake of oxLDL, we also compared oxLDL uptake in response to MG using 3,3′-dioctadecylindocarbocyanine–labeled oxLDL (Figure S1 in the online Data Supplement). Treatment of endothelial cells with MG (30 μmol/L) for 24 hours significantly increased oxLDL binding and uptake that were prevented by arginase and NOS inhibition.

Role of Peroxynitrite in MG-Induced LOX-1 Expression

Because arginase upregulation can ultimately lead to peroxynitrite formation by NOS in response to MG, we wanted to determine whether peroxynitrite was involved in the upregulation of LOX-1 in response to MG. MG (30 μmol/L) treatment for 24 hours increased LOX-1 expression in endothelial cells that was significantly reduced to control levels by FeTPPS (peroxynitrite scavenger), confirming a role for peroxynitrite in MG-induced LOX-1 expression (Figure 7B).

Discussion

In this study, we demonstrate for the first time evidence for MG formation in the vasculature of women with preeclampsia. This is supported by increased levels of CML and CEL, which are markers of MG formation in the vasculature.

Furthermore, SSAO, the enzyme that generates MG, is increased in preeclampsia, whereas the expressions of the glyoxalase enzymes that degrade MG are reduced. Moreover, the expression of GR that generates GSH is also reduced. In fact, this is the first report of AGE formation in the vasculature of women with preeclampsia. We further show that MG by upregulates LOX-1 expression via arginase.

Overexpression of glyoxalase I has been shown to inhibit AGE formation in bovine endothelial cells.[16] Our study demonstrates that decreased glyoxalase I and II expression in the vasculature of women with preeclampsia could have led to increased MG in the vasculature and, therefore, increased formation of CML and CEL. We also show an increased expression of SSAO in the vasculature of women with preeclampsia. Normally SSAO is involved in the deamination of aminoacetone[35] but in the process generates MG. Thus, we have evidence for greater production and reduced degradation of MG in the vasculature of women with preeclampsia.

MG plays a role in the development of hypertension[36] and oxidative stress.[37] It is suggested that MG may induce hypertension via different mechanisms, such as increasing vascular contractility, generating reactive oxygen species, and proliferating vascular smooth muscle in resistance arteries leading to vascular remodeling, ultimately resulting in enhanced vasoconstriction and, therefore, hypertension.[17] However, the role of MG in inducing hypertension and oxidative stress in preeclampsia is unknown. We have previously shown increased LOX-1[18] and arginase[27] expressions in the maternal vasculature of women with preeclampsia, when compared with normotensive pregnant women. We, therefore, explored the possibility that MG can affect these pathways.

Here we show that MG could be one factor involved in the upregulation of arginase and LOX-1 in preeclamptic vasculature. In response to MG, arginase inhibition significantly reduced MG-induced LOX-1 expression, suggesting a role for arginase in the upregulation of LOX-1. Importantly, in response to MG, arginase upregulation is maximal as early as 6 hours, whereas LOX-1 upregulation is maximal at 24 hours. This suggests that products generated because of arginase upregulation early in the response to MG may play a role in the upregulation of LOX-1. It is well known that NOS can generate superoxide. Our data show that increased superoxide production in response to MG is inhibitable by BEC or L-NAME to a similar extent, suggesting a role for arginase and, therefore, for NOS in possibly mediating the generation of reactive oxygen species. Inhibition of superoxide production by L-NAME suggests a role for uncoupling of NOS[34] as a source of superoxide in response to MG. In our study, we have used L-NAME as an inhibitor of all isoforms of NOS and, therefore, cannot identify the isoform of NOS that generates superoxide. Uncoupling of NOS can occur because of a deficiency of either L-arginine, the substrate, or tetrahydrobiopterin, the cofactor, depending on the isoform of NOS. Although all isoforms of NOS undergo uncoupling because of deficiency of tetrahydrobiopterin, it is primarily inducible NOS and neuronal NOS that undergo uncoupling because of L-arginine deficiency.[38–41] In our study, we show that MG can also induce peroxynitrite formation in endothelial cells. It is possible that peroxynitrite can oxidize tetrahydrobiopterin and, thus, create deficiency leading to uncoupling of NOS.[42] Thus, in addition to the direct effect of arginase upregulation on depleting L-arginine, peroxynitrite generated because of arginase upregulation can also cause uncoupling of NOS. However, further studies are needed to characterize the mechanisms of uncoupling of NOS attributed to upregulation of arginase in endothelial cells in response to MG. Because arginase inhibition with BEC reduced superoxide generation by endothelial cells in response to MG, it is reasonable to speculate that arginase could be a source of superoxide. Interestingly, MG has also been shown to inactivate human Cu, Zn superoxide dismutase that can also result in increased superoxide levels.[43]

Our data show that MG can upregulate LOX-1 in endothelial cells; therefore, MG might directly or indirectly play a role in the development of atherosclerosis in cardiovascular diseases and also in inducing such abnormalities in the vasculature of women with preeclampsia. This could also partly explain the accumulation of oxLDL in the vasculature of women with preeclampsia,[18] a feature that is analogous to atherosclerosis. Other than oxLDL, AGEs can also bind to LOX-1 and can provide a feedforward progression to induce oxidative stress via the upregulation of LOX-1.[44]

The role of MG has been extensively studied in diabetes mellitus and its complications, such as diabetic nephropathy.[5,45] This is important because renal lesion, called glomerular endotheliosis, is known to occur in preeclampsia. Because MG is involved in renal complications of diabetes mellitus, it is tempting to speculate that MG could be involved in the renal complications of preeclampsia as well. In addition, AGEs have primarily been associated with complications of diabetes mellitus, and we have now evidence to suggest that vascular complications of preeclampsia may also be attributable to AGEs. In fact, we have previously shown increased expression of receptor for AGEs in the vasculature of women with preeclampsia.[46] All of these further support a role for MG and possibly AGEs in the vascular complications and oxidative stress that are features of preeclampsia.

Perspectives

The role of MG in causing vascular complications of diabetes mellitus is well established.[5,45] The role of MG in the development of hypertension is emerging.[5,7,8,45,47–49] Diabetes mellitus, atherosclerosis, and hypertension are known risk factors for the development of preeclampsia. Therefore, factors that are involved in the above conditions may also play a role in the initiation and propagation of the disease process in preeclampsia. Our study provides evidence for increased levels of MG in the vasculature of women with preeclampsia. Moreover, novel mechanisms for MG-induced oxidative stress through arginase and LOX-1 in endothelial cells have been described. Recent studies suggest that preeclamptic women are prone to cardiovascular disease later in life.[50] Increased MG levels in the vasculature of these women might partly explain their susceptibility to develop cardiovascular complications. Our study has potential therapeutic

implications not only to prevent vascular complications of preeclampsia but also other hypertensive vascular disorders.

Acknowledgments

We thank Donna Dawson from the Royal Alexandra Hospital for sample collection.

Sources of Funding

This work was supported by grants from the Canadian Institutes for Health Research (CIHR). S.S. was supported by the Maternal-Fetal-Newborn Health and the Strategic Training Initiative in Research in Reproductive Health Sciences Training Programs of the CIHR, a full-time studentship from the Alberta Heritage Foundation for Medical Research (AHFMR), and a Junior Personnel Award from the Heart and Stroke Foundation of Canada. H.X. was supported by a summer studentship from the AHFMR. T.S. was supported in part by grants from the Ministry of Education, Culture, Sports, Science and Technology of Japan; the Ministry of Health, Labour and Welfare of Japan; the National Institute of Biomedical Innovation; Japan Science and Technology Agency; and the New Energy and Industrial Technology Development Organization. S.T.D. is an AHFMR Scientist and a Canada Research Chair in Women's Cardiovascular Health.

Disclosures

None.

References

1. Magee LA, Helewa M, Moutquin JM, von Dadelszen P, Cardew S, Cote AM, Douglas MJ, Firoz T, Gibson PS, Gruslin A, Lange I, Leduc L, Logan AG, Rey E, Senikas V, Smith GN, Bainbridge S, Chen XK, Xu H, Hutcheon J, Menzies J, Sankaralingam S, Xie F. Diagnosis, evaluation, and management of the hypertensive disorders of pregnancy. *J Obstet Gynaecol Can.* 2008;30:S1.
2. Roberts JM. Preeclampsia: what we know and what we do not know. *Semin Perinatol.* 2000;24:24–28.
3. Roberts JM. Endothelial dysfunction in preeclampsia. *Semin Reprod Endocrinol.* 1998;16:5–15.
4. Granger JP, Alexander BT, Llinas MT, Bennett WA, Khalil RA. Pathophysiology of preeclampsia: linking placental ischemia/hypoxia with microvascular dysfunction. *Microcirculation.* 2002;9:147–160.
5. Beisswenger PJ, Drummond KS, Nelson RG, Howell SK, Szwergold BS, Mauer M. Susceptibility to diabetic nephropathy is related to dicarbonyl and oxidative stress. *Diabetes.* 2005;54:3274–3281.
6. Bourajjaj M, Stehouwer CD, van Hinsbergh VW, Schalkwijk CG. Role of methylglyoxal adducts in the development of vascular complications in diabetes mellitus. *Biochem Soc Trans.* 2003;31:1400–1402.
7. Wang X, Desai K, Chang T, Wu L. Vascular methylglyoxal metabolism and the development of hypertension. *J Hypertens.* 2005;23:1565–1573.
8. Wang X, Desai K, Clausen JT, Wu L. Increased methylglyoxal and advanced glycation end products in kidney from spontaneously hypertensive rats. *Kidney Int.* 2004;66:2315–2321.
9. Vasdev S, Ford CA, Longerich L, Parai S, Gadag V, Wadhawan S. Aldehyde induced hypertension in rats: prevention by N-acetyl cysteine. *Artery.* 1998;23:10–36.
10. Chang T, Wang R, Wu L. Methylglyoxal-induced nitric oxide and peroxynitrite production in vascular smooth muscle cells. *Free Radic Biol Med.* 2005;38:286–293.
11. Wu L. The pro-oxidant role of methylglyoxal in mesenteric artery smooth muscle cells. *Can J Physiol Pharmacol.* 2005;83:63–68.
12. Ray S, Ray M. Isolation of methylglyoxal synthase from goat liver. *J Biol Chem.* 1981;256:6230–6233.
13. Casazza JP, Felver ME, Veech RL. The metabolism of acetone in rat. *J Biol Chem.* 1984;259:231–236.
14. Yu PH, Wright S, Fan EH, Lun ZR, Gubisne-Harberle D. Physiological and pathological implications of semicarbazide-sensitive amine oxidase. *Biochim Biophys Acta.* 2003;1647:193–199.
15. Kilhovd BK, Giardino I, Torjesen PA, Birkeland KI, Berg TJ, Thornalley PJ, Brownlee M, Hanssen KF. Increased serum levels of the specific AGE-compound methylglyoxal-derived hydroimidazolone in patients with type 2 diabetes. *Metabolism.* 2003;52:163–167.
16. Shinohara M, Thornalley PJ, Giardino I, Beisswenger P, Thorpe SR, Onorato J, Brownlee M. Overexpression of glyoxalase-I in bovine endothelial cells inhibits intracellular advanced glycation endproduct formation and prevents hyperglycemia-induced increases in macromolecular endocytosis. *J Clin Invest.* 1998;101:1142–1147.
17. Chang T, Wu L. Methylglyoxal, oxidative stress, and hypertension. *Can J Physiol Pharmacol.* 2006;84:1229–1238.
18. Sankaralingam S, Xu Y, Sawamura T, Davidge ST. Increased lectin-like oxidized low-density lipoprotein receptor-1 expression in the maternal vasculature of women with preeclampsia: role for peroxynitrite. *Hypertension.* 2009;53:270–277.
19. Sawamura T, Kume N, Aoyama T, Moriwaki H, Hoshikawa H, Aiba Y, Tanaka T, Miwa S, Katsura Y, Kita T, Masaki T. An endothelial receptor for oxidized low-density lipoprotein. *Nature.* 1997;386:73–77.
20. Cominacini L, Rigoni A, Pasini AF, Garbin U, Davoli A, Campagnola M, Pastorino AM, Lo Cascio V, Sawamura T. The binding of oxidized low density lipoprotein (ox-LDL) to ox-LDL receptor-1 reduces the intracellular concentration of nitric oxide in endothelial cells through an increased production of superoxide. *J Biol Chem.* 2001;276:13750–13755.
21. Noris M, Todeschini M, Cassis P, Pasta F, Cappellini A, Bonazzola S, Macconi D, Maucci R, Porrati F, Benigni A, Picciolo C, Remuzzi G. L-arginine depletion in preeclampsia orients nitric oxide synthase toward oxidant species. *Hypertension.* 2004;43:614–622.
22. Li H, Meininger CJ, Hawker JR Jr, Haynes TE, Kepka-Lenhart D, Mistry SK, Morris SM Jr, Wu G. Regulatory role of arginase I and II in nitric oxide, polyamine, and proline syntheses in endothelial cells. *Am J Physiol Endocrinol Metab.* 2001;280:E75–E82.
23. Waddington S, Cook HT, Reaveley D, Jansen A, Cattell V. L-arginine depletion inhibits glomerular nitric oxide synthesis and exacerbates rat nephrotoxic nephritis. *Kidney Int.* 1996;49:1090–1096.
24. Xu W, Kaneko FT, Zheng S, Comhair SA, Janocha AJ, Goggans T, Thunnissen FB, Farver C, Hazen SL, Jennings C, Dweik RA, Arroliga AC, Erzurum SC. Increased arginase II and decreased NO synthesis in endothelial cells of patients with pulmonary arterial hypertension. *FASEB J.* 2004;18:1746–1748.
25. Xia Y, Dawson VL, Dawson TM, Snyder SH, Zweier JL. Nitric oxide synthase generates superoxide and nitric oxide in arginine-depleted cells leading to peroxynitrite-mediated cellular injury. *Proc Natl Acad Sci U S A.* 1996;93:6770–6774.
26. Vasquez-Vivar J, Kalyanaraman B, Martasek P, Hogg N, Masters BS, Karoui H, Tordo P, Pritchard KA Jr. Superoxide generation by endothelial nitric oxide synthase: the influence of cofactors. *Proc Natl Acad Sci U S A.* 1998;95:9220–9225.
27. Sankaralingam S, Davidge ST. Role of arginase in the pathophysiology of preeclampsia [abstract]. *FASEB J.* 2008;22:758.755.
28. Koito W, Araki T, Horiuchi S, Nagai R. Conventional antibody against Nepsilon-(carboxymethyl)lysine (CML) shows cross-reaction to Nepsilon-(carboxyethyl)lysine (CEL): immunochemical quantification of CML with a specific antibody. *J Biochem.* 2004;136:831–837.
29. Ahmed MU, Brinkmann Frye E, Degenhardt TP, Thorpe SR, Baynes JW. N-epsilon-(carboxyethyl)lysine, a product of the chemical modification of proteins by methylglyoxal, increases with age in human lens proteins. *Biochem J.* 1997;324(pt 2):565–570.
30. McLellan AC, Phillips SA, Thornalley PJ. The assay of methylglyoxal in biological systems by derivatization with 1,2-diamino-4,5-dimethoxybenzene. *Anal Biochem.* 1992;206:17–23.
31. Wang H, Meng QH, Gordon JR, Khandwala H, Wu L. Proinflammatory and proapoptotic effects of methylglyoxal on neutrophils from patients with type 2 diabetes mellitus. *Clin Biochem.* 2007;40:1232–1239.
32. Shamsi FA, Partal A, Sady C, Glomb MA, Nagaraj RH. Immunological evidence for methylglyoxal-derived modifications in vivo: determination of antigenic epitopes. *J Biol Chem.* 1998;273:6928–6936.
33. Corraliza IM, Campo ML, Soler G, Modolell M. Determination of arginase activity in macrophages: a micromethod. *J Immunol Methods.* 1994;174:231–235.
34. Taylor NE, Maier KG, Roman RJ, Cowley AW Jr. NO synthase uncoupling in the kidney of Dahl S rats: role of dihydrobiopterin. *Hypertension.* 2006;48:1066–1071.
35. Deng Y, Yu PH. Assessment of the deamination of aminoacetone, an endogenous substrate for semicarbazide-sensitive amine oxidase. *Anal Biochem.* 1999;270:97–102.

36. Vasdev S, Gill V, Singal P. Role of advanced glycation end products in hypertension and atherosclerosis: therapeutic implications. *Cell Biochem Biophys*. 2007;49:48–63.
37. Desai KM, Wu L. Free radical generation by methylglyoxal in tissues. *Drug Metabol Drug Interact*. 2008;23:151–173.
38. Bevers LM, Braam B, Post JA, van Zonneveld AJ, Rabelink TJ, Koomans HA, Verhaar MC, Joles JA. Tetrahydrobiopterin, but not L-arginine, decreases NO synthase uncoupling in cells expressing high levels of endothelial NO synthase. *Hypertension*. 2006;47:87–94.
39. Cardounel AJ, Xia Y, Zweier JL. Endogenous methylarginines modulate superoxide as well as nitric oxide generation from neuronal nitric-oxide synthase: differences in the effects of monomethyl- and dimethyl-arginines in the presence and absence of tetrahydrobiopterin. *J Biol Chem*. 2005;280:7540–7549.
40. Xia Y, Roman LJ, Masters BS, Zweier JL. Inducible nitric-oxide synthase generates superoxide from the reductase domain. *J Biol Chem*. 1998;273: 22635–22639.
41. Xia Y, Tsai AL, Berka V, Zweier JL. Superoxide generation from endothelial nitric-oxide synthase. A Ca2+/calmodulin-dependent and tetrahydrobiopterin regulatory process. *J Biol Chem*. 1998;273: 25804–25808.
42. Milstien S, Katusic Z. Oxidation of tetrahydrobiopterin by peroxynitrite: implications for vascular endothelial function. *Biochem Biophys Res Commun*. 1999;263:681–684.
43. Kang JH. Modification and inactivation of human Cu, Zn-superoxide dismutase by methylglyoxal. *Mol Cells*. 2003;15:194–199.
44. Inoue N, Sawamura T. Lectin-like oxidized LDL receptor-1 as extracellular chaperone receptor: its versatile functions and human diseases. *Methods*. 2007;43:218–222.
45. Mostafa AA, Randell EW, Vasdev SC, Gill VD, Han Y, Gadag V, Raouf AA, El Said H. Plasma protein advanced glycation end products, carboxymethyl cysteine, and carboxyethyl cysteine, are elevated and related to nephropathy in patients with diabetes. *Mol Cell Biochem*. 2007;302: 35–42.
46. Cooke CL, Brockelsby JC, Baker PN, Davidge ST. The receptor for advanced glycation end products (RAGE) is elevated in women with preeclampsia. *Hypertens Pregnancy*. 2003;22:173–184.
47. Wang X, Chang T, Jiang B, Desai K, Wu L. Attenuation of hypertension development by aminoguanidine in spontaneously hypertensive rats: role of methylglyoxal. *Am J Hypertens*. 2007;20:629–636.
48. Wu L. Is methylglyoxal a causative factor for hypertension development? *Can J Physiol Pharmacol*. 2006;84:129–139.
49. Wu L, Juurlink BH. Increased methylglyoxal and oxidative stress in hypertensive rat vascular smooth muscle cells. *Hypertension*. 2002;39: 809–814.
50. Craici I, Wagner S, Garovic VD. Preeclampsia and future cardiovascular risk: formal risk factor or failed stress test? *Ther Adv Cardiovasc Dis*. 2008;2:249–259.

LOX-1 augments oxLDL uptake by lysoPC-stimulated murine macrophages but is not required for oxLDL clearance from plasma

David F. Schaeffer,[1,*] Maziar Riazy,[1,*] Kuljit S. Parhar,[*] Johnny H. Chen,[*] Vincent Duronio,[*] Tatsuya Sawamura,[†] and Urs P. Steinbrecher[2,*]

Department of Medicine,[*] University of British Columbia, Vancouver, Canada; Department of Vascular Physiology,[†] National Cardiovascular Research Institute, Osaka, Japan

Abstract **Oxidized LDL (oxLDL) promotes lipid accumulation as well as growth and survival signaling in macrophages. OxLDL uptake is mainly due to scavenger receptors SR-AI/II and CD36. However, other scavenger receptors such as lectin-like oxLDL receptor-1 (LOX-1) may also play a role. We used mice with targeted inactivation of the LOX-1 gene to define the role of this receptor in the uptake of oxLDL and in activation of survival pathways. There was no difference in uptake or degradation of ^{125}I-oxLDL in unstimulated macrophages from wild-type and LOX-1 knockout mice and no difference in the rate of clearance of oxLDL from plasma in vivo. However, when expression of LOX-1 was induced with lysophosphatidylcholine, oxLDL uptake and degradation increased 2-fold in wild-type macrophages but did not change in LOX-1 knockout macrophages. Macrophages lacking LOX-1 showed the same stimulation of PKB phosphorylation and enhancement of survival by oxLDL as wild-type cells. These data show that LOX-1 does not alter the uptake of oxLDL in unstimulated macrophages and is not essential for the pro-survival effect of oxLDL in these cells. However, LOX-1 expression is highly inducible by lysophosphatidylcholine and pro-inflammatory cytokines, and if that occurred in macrophages within atheromas, LOX-1 could substantially increase oxLDL uptake by lesion macrophages.**—Schaeffer, D. F., M. Riazy, K. S. Parhar, J. H. Chen, V. Duronio, T. Sawamura, and U. P. Steinbrecher. **LOX-1 augments oxLDL uptake by lysoPC-stimulated murine macrophages but is not required for oxLDL clearance from plasma.** ***J. Lipid Res.*** **2009. 50: 1676–1684.**

Supplementary key words apoptosis • lysophosphatidycholine • macrophage • oxidized low density lipoprotein • scavenger receptor

The lectin-like oxidized LDL receptor (LOX-1) is a 50 kDa type II membrane receptor belonging to the C-type lectin family. It is expressed in vascular smooth muscle cells, macrophages, fibroblasts, and platelets (1, 2). It is reported to be upregulated in pathological conditions including hypertension, diabetes, and atherosclerosis. The potential role of LOX-1 in atherosclerotic process has been based on a number of observations. LOX-1 has the capability to bind, internalize, and degrade oxLDL (3). The activation of LOX-1 by oxLDL induces endothelial dysfunction and apoptosis (4–6). Furthermore LOX-1 is present in atheroma-derived cells and has been identified in animal and human atherosclerotic lesions in vivo (7, 8). Mehta et al. recently reported that in LDL receptor knockout mice, LOX-1 gene inactivation reduces the extent of atherosclerosis (9). The LOX-1 receptor has also been shown to mediate intracellular cell signaling events. For example, the binding of oxLDL to LOX-1 is reported to activate signaling via ERK that modulates the Bax/Bcl2 ratio in vascular smooth muscle cells and to activate NF- B in endothelial cells (10).

LOX-1 is a member of the scavenger receptor family of multiligand receptors that are thought to play a role in innate immunity (11). Other members of this family expressed in macrophages include SRAI/II, CD36, macrosialin/CD68, macrophage receptor with collagenous structure (MARCO), scavenger receptor expressed in endothelial cells (SREC), and a transmembrane chemokine and receptor for phosphatidylserine and oxLDL, SR-PSOX/CXCL16 (11). Previous studies indicate that 30–40% of the degradation of extensively oxidized LDL by

This study was supported by grants from the Canadian Institutes of Health Research (U.P.S.) and the Heart and Stroke Foundation of British Columbia and Yukon (U.P.S. and V.D.); a fellowship from the Canadian Institutes of Health Research/Michael Smith Foundation for Health Research (D.F.S.); and a studentship from the Canadian Liver Foundation (K.S.P.).

Manuscript received 8 April 2009.

Published, JLR Papers in Press, April 9, 2009
DOI 10.1194/jlr.M900167-JLR200

Abbreviations: acLDL, acetylated low density lipoprotein; BMDM, bone marrow derived macrophages; lysoPC, lysophosphatidycholine; M-CSF, macrophage colony-stimulating factor; MTS, 3-(4,5-dimethylthiazol-2-yl)-5-(3-carboxymethoxyphenyl)-2-(4-sulfophenyl)-2*H*-tetrazolium, inner salt; oxLDL, oxidized low density lipoprotein.

[1]D. F. Schaeffer and M. Riazy contributed equally to this work.
[2]To whom correspondence should be addressed.
e-mail: usteinbr@interchange.ubc.ca

mouse peritoneal macrophages is mediated by SR-AI/II and that CD36 accounts for an additional 35% of oxLDL degradation (12, 13). In peritoneal macrophages from mice lacking both SRAI/II and CD36, degradation of oxLDL was reduced by 75% (13). It has been suggested that LOX-1 may also be an important receptor for oxLDL in macrophages (14), but to date no studies have provided a quantitative estimate of the contribution of LOX-1 to oxLDL uptake by macrophages.

We recently showed that oxidized LDL blocks apoptosis in macrophages through activation of the phosphatidylinositol 3-kinase/protein kinase B (PI3K/PKB) cascade, translocation of NF- B to the nucleus, and induction of the anti-apoptotic factor $BclX_L$ (15, 16). Our preliminary results in SR-AI/II macrophages (17) and CD36 knockout macrophages (unpublished) suggest that the anti-apoptotic effect of oxLDL does not require either of these two scavenger receptors. LOX-1 was deemed an attractive candidate because its much higher affinity for oxidized LDL compared with acetyl LDL or native LDL is congruent with the finding that oxLDL (but not acetyl LDL or native LDL) can inhibit apoptosis in macrophages and because it has been shown to be involved in survival signaling and NF- B activation (4, 6, 18).

In the present study we describe results of experiments using LOX-1 knockout mice to examine the role the LOX-1 receptor plays in mediating uptake of, and signaling by, ox-LDL in macrophages.

MATERIALS AND METHODS

Materials

Carrier-free Na ^{125}I was purchased from Perkin Elmer (Woodbridge, Ontario). DMEM, αMEM medium, propidium iodide, and RNase A were obtained from Invitrogen (Burlington, ON, Canada). Defined fetal bovine serum (FBS) was from HyClone (Logan, UT). Promega (Madison, WI) supplied 3-(4,5-Dimethylthiazol-2-yl)-5-(3-carboxymethoxyphenyl)-2-(4-sulfophenyl)-2*H*-tetrazolium, inner salt (MTS). Phenazine methosulfate (PMS) and 1-stearoyl lysophosphatidylcholine were from Sigma Aldrich (St. Louis, MO). Centriplus 20 ultrafilters were purchased from Amicon (Beverly, MA). Molecular Probes (Eugene OR) provided 1,1′-dioctadecyl-3,3,3′,3′-tetramethylindocarbocyanine perchlorate (DiI). Anti-CD68 was purchased from Serotec (Raleigh, NC). Primary antibody against p85 subunit of PI3K was purchased from Santa Cruz Biotechnology (Santa Cruz, CA). Antibodies against total and phosphorylated PKB (Ser470) were from Cell Signaling Technology (Beverly, MA).

Animals

Inactivation of the single-copy murine LOX-1 receptor gene by homologous recombination was performed in the laboratory of Dr. T. Sawamura (9). Offspring with the inactivated gene in germine cells were backcrossed 8 times onto a C57bl/6 background. LOX-1 genotypes were verified by PCR analysis of tail DNA in all breeding animals, as well as in selected experimental animals. DNA was extracted using a Qiagen DNeasy kit. The forward primer for the LOX-1 deletion was 5′-CAGCGAACACAGCTCCGTCTTGAAGG-3′ and the reverse primer was 5′-GGCCAACCATGGCTTGGGAGAATGG-3′. The forward primer for the neomycin-resistance cassette was 5′-CAACGCTATGTCCTGATAGCGGTCC-3′ and the reverse primer was 5′-CGTGTTCCGGCTGTCAGCGCAGG-3′. Wild-type C57bl/6 mice were purchased from The Jackson Laboratory. All animal procedures were in accordance with the guidelines of the Canadian Council on Animal Care and were approved by the Animal Care Committee of the University of British Columbia.

Lipoprotein isolation and labeling

LDL (d = 1.019–1.063 g/ml) was isolated by sequential ultracentrifugation of EDTA-anticoagulated fasting plasma obtained from healthy normolipidemic volunteers (19). Radioiodination was performed using a modification of the iodine monochloride method of MacFarlane (20). The specific activity was between 100 and 150 cpm/ng LDL protein. Iodination was performed before oxidation or acetylation of LDL. Lipoprotein-deficient serum (LPDS) was prepared from the d > 1.25 fraction.

LDL modification

LDL was oxidized by incubating 200 μg/ml LDL in PBS containing 5 μmol/L $CuSO_4$ at 37°C for 20 h (21). OxLDL was then washed and concentrated to about 1 mg/ml with Centriplus 20 ultrafilters (Millipore, Bedford, MA). Agarose gel electrophoresis typically showed a 4-fold increase in electrophoretic mobility for oxidized LDL compared with native LDL. LDL was acetylated by adding four 1-μl aliquots of acetic anhydride at 10 min intervals to 2 mg of LDL in 600 μl of ice-cold 50% saturated sodium acetate (22).

Macrophage isolation and culture

Peritoneal macrophages were obtained from wild-type or LOX-1 knockout C57/bl mice by peritoneal lavage with ice-cold Ca^{2+}-free Dulbecco's PBS. Macrophages were suspended in α-minimal essential medium (α-MEM) with 10% fetal bovine serum (FBS) and plated in 12-well plastic culture plates. Nonadherent cells were removed by medium exchange after 1 h. Adherent macrophages were cultured overnight, washed with α-MEM, and then used for experiments. Bone marrow cells were isolated from the femurs of 6–8-week-old female C57/bl mice as described previously (22). Cells were plated for 24 h in RPMI 1640 containing 10% FBS and 10% L-cell conditioned medium as the source of M-CSF. The nonadherent cells were removed and cultured in the above medium for 5–7 days until 80% confluence was reached.

Reverse transcription polymerase chain reaction analysis

RNA was isolated from BMDM and peritoneal macrophages (PM) from wild-type or LOX-1 knockout mice using Trizol (Invitrogen, Burlington, ON). Total RNA was then used as a template for first strand cDNA synthesis using M-MLV reverse transcriptase from Promega (Madison, WI) according to the manufacturer's instructions. The resulting cDNA was amplified using the forward primer 5′-CGTGTTCCGGCTGTCAGCGCAGG-3′ and the reverse primer 5′-CAACGCTATGTCCTGATAGCGGTCC-3′. These sequences were obtained from the genomic sequence using the algorithm Primer 3 (www-genome.wi.mit.edu/cgi-bin/primer/primer3_www.cgi). PCR was performed with Taq DNA polymerase (Invitrogen, Burlington, ON) in a 25 μl reaction volume containing 10 pmol of each primer. Amplification was performed for 35 cycles at 94°C for 2 min, 94°C for 40s, 60°C for 1 min, and 72°C for 1 min. The final elongation phase was done at 72°C for 10 min. The PCR products were electrophoresed on a 1.5% agarose gel and visualized using ethidium bromide under UV light.

Fluorescent labeling

Fluorescent labeling of oxLDL was performed by adding 100 μg DiI in 60μl dimethyl sulfoxide to 2 mg of oxLDL in the pres-

ence of d > 1.21g/ml plasma fraction as a source of lipid transfer activity (24). Following an 8 h incubation period at 37°C, the labeled oxLDL was reisolated by ultracentrifugation at d = 1.1. This procedure typically resulted in an incorporation of 5–15 μg of DiI per mg of LDL protein.

Assays of LDL uptake and degradation in cultured cells

Macrophages were incubated at 37°C with varying concentrations of radioiodinated native, oxidized, or acetylated LDL in α-MEM with 2.5% lipoprotein deficient serum. After 4 h, the medium was removed and the cells were washed. LDL degradation products were quantified by mixing 1 ml of the supernatant medium with 350 μl of 50% trichloroacetic acid and 350 μl of 7.5% $AgNO_3$. The mixture was centrifuged at 2500 rpm for 15 min, and the supernatant was counted on a LKB 1282 γ counter. The cells were removed from the plates with Teflon cell lifters and counted to determine cell-associated LDL.

Uptake of DiI labeled oxLDL by macrophages

Peritoneal macrophages were incubated for 5 h at 37°C with 10 μg/ml DiI-labeled oxidized LDL in α-MEM containing 2.5% LPDS. Cells were washed with PBS, fixed with 2% formaldehyde, and mounted in 90% glycerol, 9.75% PBS, and 0.25% 1,4-diazabicyclo[2,2,2]octane. Cells were examined with a Zeiss Axioskop fluorescence microscope in epifluorescent mode with a fluorescein filter set.

In vivo clearance of LDL

Clearance of oxLDL or native LDL was measured as previously described (25). Briefly, wild-type or LOX-1 deficient mice were anesthetized with 2% isoflurane. The external jugular vein was exposed with the aid of a Zeiss operating microscope (Carl Zeiss Canada Ltd., Don Mills, Ontario) and cannulated with a PE 10 polyethylene catheter (outer diameter 0.61 mm; VWR Canlab), positioned with its tip in the superior vena cava. ^{125}I oxLDL (1-2 million cpm) in 200 μl of 150 mM NaCl was drawn into a 1ml syringe. The syringe was counted before and after the injection to allow an accurate determination of the amount of radioactivity administered. Five or six 20 μl blood samples were collected over 20 min. A second injection was then performed with a similar amount of native LDL, and four or five 20 μl samples were collected over 20 min. For oxLDL, the concentration at zero time was calculated using the injected dose of oxLDL and the volume of distribution of native LDL.

Cell viability assay

Macrophage survival was determined by the MTS-formazan method. This assay is based on the cellular bioreduction of MTS by mitochondrial dehydrogenase enzymes in metabolically active cells. The quantity of formazan product formed was measured by the absorbance at 490 nm and is directly proportional to the number of viable cells in culture (26). MTS-PMS solution (20 μl/well) was added to wells containing 100 μl of culture medium in 96 well plates for 3 h before terminating the experiment. This resulted in final MTS and PMS concentrations of 333 μg/ml and 25 μM, respectively. After 3 h incubation at 37°C in a humidified 5% CO_2 atmosphere, the absorbance at 490 nm was recorded with an ELISA plate reader.

Apoptosis assay

Propidium iodide staining and FACS analysis was used to quantitate the subdiploid population. At the end of 24 hr incubation, BMDM from wild-type or LOX-1 knockout mice were fixed and permeabilized with ethanol 70% (v/v) for 1 h at 4°C and washed twice in PBS containing 0.01% glucose. Cells were then resuspended in the same buffer plus RNase A (final concentration 0.1 mg/ml) and propidium iodide (final concentration 0.12 mg/ml). Fluorescence was measured with a BD FACS Canto. The data was analyzed with FCS Express Pro Software Version 3 (De Novo Software, Thornhill, Canada) with gating to exclude debris and cellular aggregates.

Immunoblotting

BMDM were harvested as described above and lysed in ice-cold homogenization buffer [20 mM morpholinepropanesulfonic acid, pH 7.2, 1% Triton X-100, 50 mM β-glycerol phosphate, 5 mM EGTA, 2 mM EDTA, 1 mM sodium vanadate, 25 μM β-methyl aspartic acid, 1 mM DTT, 1 mM phenylmethylsulfonyl fluoride, aprotinin (10 μg/ml), and leupeptin (10 μg/ml)]. Lysates were centrifuged at 14,000 rpm for 10 min, and the protein content of supernatants was quantified using the Bradford protein assay. Fifty micrograms of protein from each sample was loaded and separated by SDS-PAGE using a 10% separating gel. Gels were calibrated with prestained SDS-PAGE low molecular weight standards (Bio-Rad, Hercules, CA). Proteins were then transferred to nitrocellulose membranes which were then blocked for 1 h with 4% skim milk, 0.01% NaN_3 in TBS-0.1% Tween 20. The membranes were cut at about the 70 kDa point, and the bottom section was then incubated with anti-phospho(Ser473) PKB antibody overnight in TBS-0.1% Tween 20 at 4°C, washed three times, and then incubated with horseradish peroxidase-conjugated secondary antibody at a 1:5,000 dilution for 1 h. The bands were then visualized by enhanced chemiluminescence. This blot was then stripped in Tris buffer containing SDS (2%) and β-2-mercaptoethanol (100 mM) at 50°C for 20 min, washed, and reprobed with antibody to PKB. The top section of the membrane was incubated with antibody against the p85 subunit of PI3K, and bands were visualized as above.

Analytic procedures

LDL and cell protein was assayed by the method of Lowry (27) in the presence of 0.05% sodium deoxycholate with BSA as the standard. Lipoprotein electrophoresis was done using the Titan gel lipoprotein electrophoresis system (Intermedico, Markham, Ontario). Lipoprotein bands were visualized by staining with Fat red.

Statistical analysis

Statistical analysis was done using ANOVA or Student's *t*-test as appropriate. $P < 0.05$ was taken as significant.

RESULTS

LOX-knockout mice

Homozygous LOX-1 deficient animals had no overt phenotype and were fertile. The absence of LOX-1 mRNA was verified by RT-PCR (**Fig. 1**).

Uptake of fluorescently labeled oxLDL by macrophages

The lipophilic fluorophore diI crosses lysosomal membranes very slowly and so serves as a cumulative marker of the quantity of labeled LDL that is internalized by cells (24, 28). To obtain a morphologic comparison of the internalization of oxLDL in control and LOX-1 deficient macrophages, we incubated peritoneal macrophages grown on coverslips for 5 h with diI-labeled oxLDL. Fluorescence micrographs indicate that there was no apparent difference in the intensity or distribution of fluorescence between wild-type and LOX-1 deficient cells (**Fig. 2**).

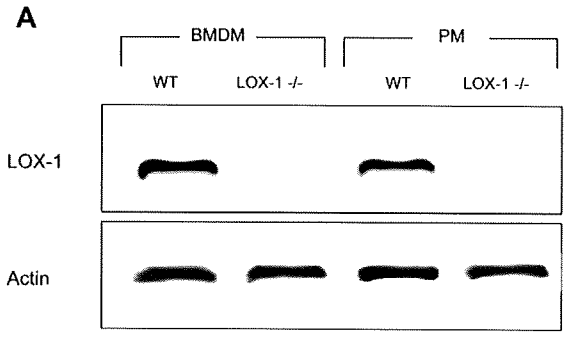

Fig. 1. Absence of LOX-1 mRNA in macrophages harvested from LOX-1 knockout mice. Absence of LOX-1 mRNA in knockout animals was verified by RT-PCR of total RNA from bone marrow derived macrophages (BMDM) or peritoneal macrophages (PM). An amplicon with migration consistent with the predicted nucleotide sequence is seen in the wild-type cells, whereas no band is seen in knockout cells.

Uptake and degradation of modified LDLs in wild-type and LOX-1 deficient peritoneal macrophages

To quantify the relative rates of oxLDL uptake, we incubated macrophages for 5 h with radioiodinated native LDL, oxLDL, or acetyl LDL and then measured rates of LDL uptake and degradation. There was no difference in the rate of uptake of native LDL or either modified LDL in wild-type compared with LOX-1 knockout peritoneal macrophages (**Fig. 3**).

Uptake and degradation of oxLDL in wild-type and LOX-1 deficient peritoneal macrophages

Different scavenger receptors are known to have different affinities for minimally, moderately, or extensively oxidized LDL. We therefore tested the uptake and degradation of radioactively labeled oxLDL in LOX-1 deficient and wild-type macrophages. There was no difference between wild-type and LOX-1 deficient macrophages in uptake or degradation of minimally, moderately, or extensively oxidized LDL (**Fig. 4**).

Effect of induction of LOX-1 gene expression on oxLDL uptake and degradation in wild-type macrophages

LOX-1 has been shown to mediate uptake and degradation of oxLDL in endothelial cells, smooth muscle cells, and in transfected cell lines. Hence, it seemed possible that the failure to detect a difference between wild-type and LOX-1 deficient macrophages might be because a high level of expression of SRAI/II and CD36 masked the contribution of LOX-1. To test this, we took advantage of the observation that lysophosphatidylcholine causes a marked and selective (up to 5-fold) induction of LOX-1 in endothelial cells and smooth muscle cells (29, 30). Cultured peritoneal macrophages from wild-type and LOX-1 deficient mice were preincubated for 12 h with varying concentrations of lysophosphatidylcholine, and then incubated for 5 h with ^{125}I oxLDL or ^{125}I LDL (**Fig. 5A**, 5B). Lysophosphatidylcholine caused a concentration-dependent increase in oxLDL uptake and degradation in wild-type macrophages but had no effect on uptake and

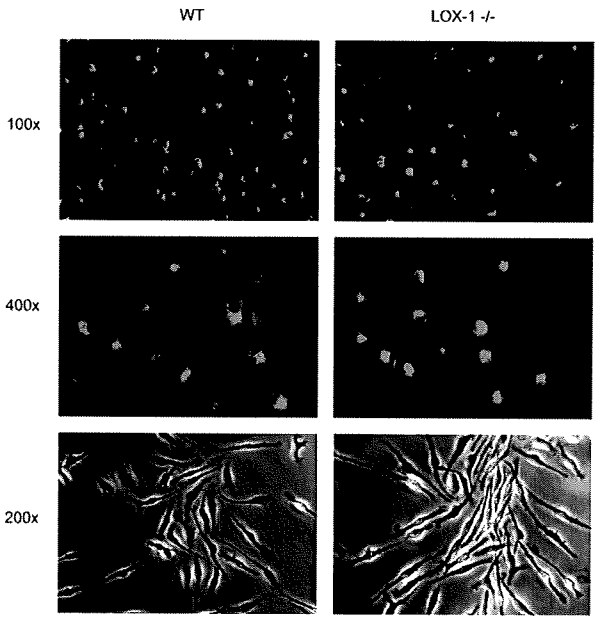

Fig. 2. Uptake of oxLDL in peritoneal macrophages. Resident peritoneal macrophages from wild-type (WT) and LOX-1 knockout mice were incubated for 5 h with 10μg/ml DiI-labeled oxidized LDL, and then examined using a Zeiss Axioskop fluorescence microscope. No difference in fluorescence intensity is seen.

degradation in LOX-1 deficient cells. These concentrations of lysophosphatidylcholine are the same as those reported to induce LOX-1 expression in smooth muscle cells and endothelial cells (29). The upregulation of LOX-1 mRNA by these concentrations of lysophosphatidylcholine was confirmed by RT-PCR (Fig. 5C).

In vivo clearance of oxLDL

To directly assess the role of LOX-1 in oxLDL clearance in vivo, we compared the rates at which oxLDL was removed from plasma from wild-type and LOX-1 deficient mice. Animals were injected first with ^{125}I-oxLDL and then

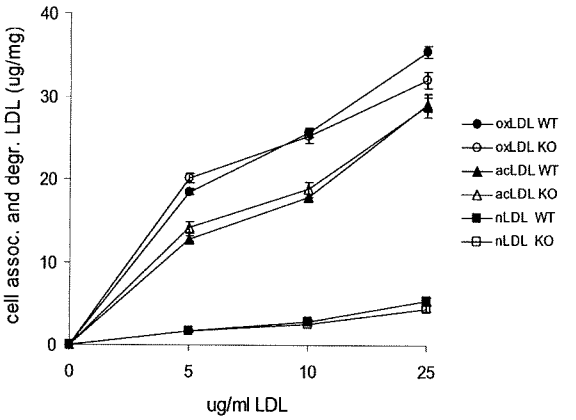

Fig. 3. Uptake and degradation of native, oxidized, and acetylated LDL in macrophages. Cultured peritoneal macrophages from wild-type mice (solid symbols) or knockout mice (open symbols) were incubated with the indicated concentration of ^{125}I-labeled native LDL, oxLDL, or acetyl LDL.

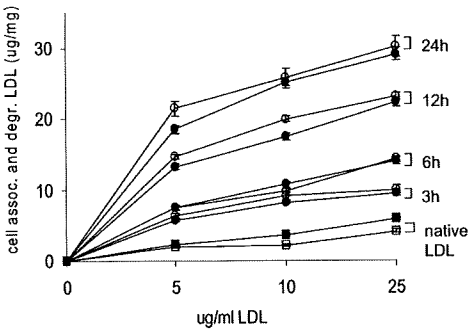

Fig. 4. Uptake and degradation of LDL oxidized to various degrees in wild-type and LOX-1 deficient peritoneal macrophages. Cultured peritoneal macrophages from wild-type mice (solid symbols) or knockout mice (open symbols) were incubated with the indicated concentration of native ^{125}I-LDL (squares) or ^{125}I-LDL oxidized by exposure to 5μM Cu^{2+} for 3 h, 6 h, 12 h, or 24 h (circles). The electrophoretic mobility of oxLDL was 1.0 (3 h), 1.3 (6 h), 2.2 (12 h) or 3.8 (24 h) times that of native LDL. After 5 h, cells and media were assayed for uptake and degradation of labeled lipoprotein. Results are the sum of cell-associated and degraded LDL expressed as μg LDL per mg cell protein. Values are the means +/− SEM of triplicates.

with native ^{125}I-LDL and serial blood samples were assayed for radioactivity. The rates of plasma clearance of oxLDL were very rapid and indistinguishable between wild-type and LOX-1 deficient animals (**Fig. 6**).

Role of LOX-1 in the ability of oxLDL to increase survival of BMDM

We have shown that oxLDL promotes growth and cytokine-independent survival in macrophages at least in part by activating the PI3K/PKB pro-survival pathway (15–17 26). We previously found that oxLDL promoted survival in SRAI/II-deficient macrophages (31) and in CD36-deficient macrophages (unpublished), so we hypothesized that LOX-1 might be the receptor required for PKB activation. To address this, we compared the ability of oxLDL to promote survival in cytokine-deprived BMDM from wild-type and LOX-1 deficient mice. After 24 h there was no significant difference in the viability of wild-type and LOX-1 deficient cells treated with oxLDL (**Fig. 7A**). There was no significant difference between wild-type and LOX-1 BMDM in the percentage of sub-diploid cells after incubation with oxLDL (Fig. 7B). Deficiency of LOX-1 did not abolish the ability of oxLDL to promote PKB phosphorylation in BMDM (**Fig. 8**).

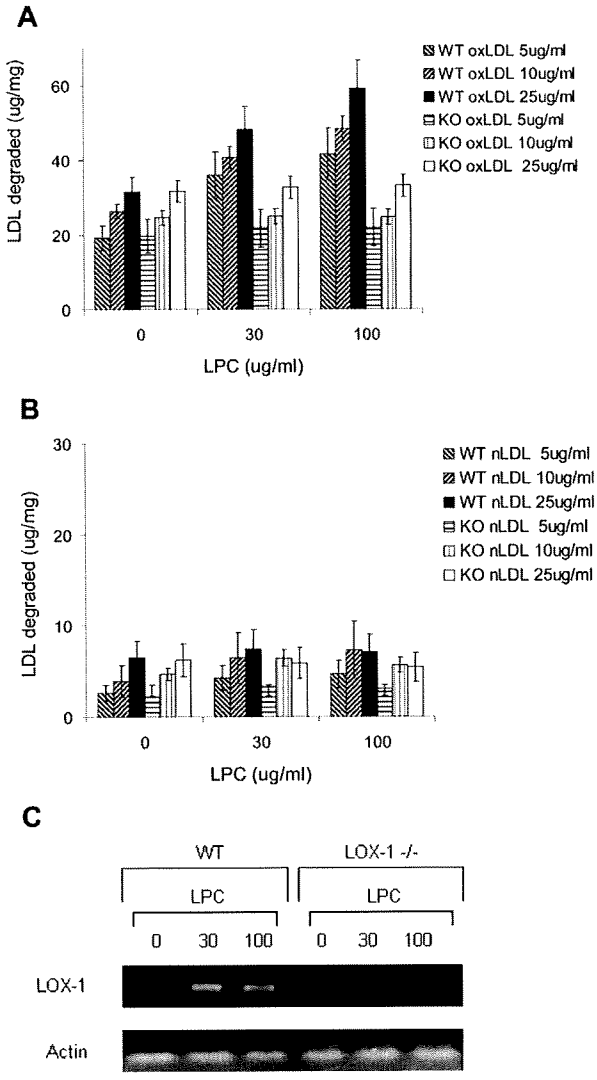

Fig. 5. Effect of induction of LOX-1 with lysophosphatidylcholine on oxLDL uptake and degradation. Cultured peritoneal macrophages from wild-type and LOX-1 knockout mice were preincubated for 12 h with 0, 30, or 100 ug/ml lysophosphatidylcholine. Cells were then washed and incubated for 5 h with varying concentrations of ^{125}I-oxLDL (A) or ^{125}I-LDL (B). Values shown are means ± SD of the sum of cell-associated and degraded oxLDL, reflecting total oxLDL uptake during the incubation. (C) RT-PCR blot showing that LOX-1 mRNA expression was increased in wild-type macrophages by these concentrations of lysophosphatidylcholine.

DISCUSSION

The studies described in this report address two different aspects of the interaction of oxLDL with LOX-1 in macrophages. The first issue is the role of LOX-1 in uptake and degradation of oxLDL by macrophages. LOX-1 clearly has the ability to bind and internalize LDL in endothelial cells and in CHO cells transfected with LOX-1 receptor constructs (3). LOX-1 has a similar ligand specificity as SR-AI/II and CD36, although its affinity for oxLDL is substantially higher than its affinity for acetyl LDL (31). We previously showed that about 70% of the uptake of oxLDL in macrophages was not due to SRAI/II (12). Competition experiments indicated that polyinosinic acid, but not acetyl LDL or native LDL, blocked the SRAI/II-independent uptake of oxidized LDL (12). Although CD36 has been shown to contribute to oxLDL uptake in macrophages, our preliminary findings in CD36 −/− macrophages showed no reduction in the anti-apoptotic effect of oxLDL. Hence it seemed possible that some of the SRAI/II and CD36-independent uptake might be due to a receptor such as LOX-1. This receptor has a reported

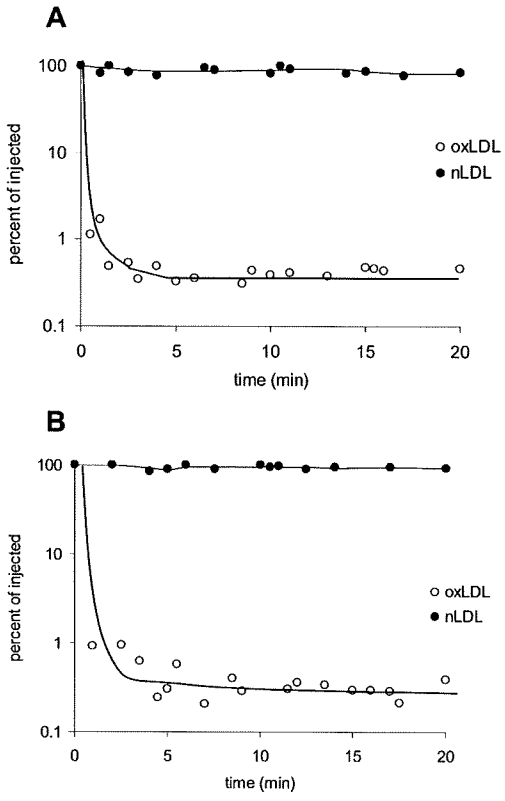

Fig. 6. In vivo plasma clearance of oxidized and native LDL in wild-type and LOX-1 deficient mice. Wild-type mice (A, n = 3) or LOX-1 knockout mice (B, n = 3) were anesthetized with 2% isoflurane. Oxidized ^{125}I LDL (open circles) or native ^{125}I LDL (solid circles) was injected through a cannula placed in the internal jugular vein. Serial 20 μl blood samples were withdrawn at the indicated time points and radioactivity was measured. Points for all three animals in each case are plotted together. The electrophoretic mobility of oxLDL in this experiment was 4.1-fold that of native LDL.

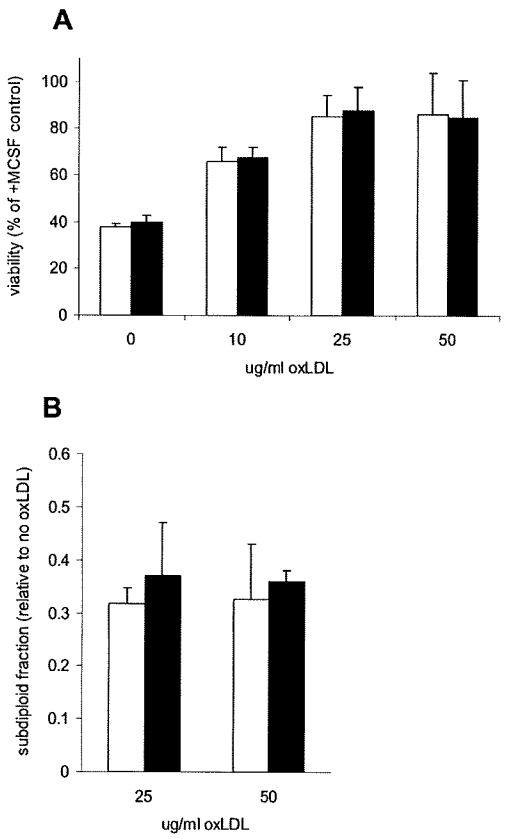

Fig. 7. LOX-1 deficiency does not impair the ability of oxLDL to inhibit macrophage apoptosis. (A) BMDM from wild-type mice (open bars) or LOX-1 −/− mice (solid bars) were seeded at 3 × 10^3 cells/well in 96 well plates and cultured for 24 h. They were then washed and incubated for 24 h without M-CSF but with the indicated concentrations of ox-LDL. Viability was then measured by the bioreduction of MTS (described in Materials and Methods) and expressed as a percentage of that in control cells treated with M-CSF. (B) BMDM were plated at 10^6 cells/well in six well plates and incubated for 24 h in medium containing indicated concentration of oxLDL but no M-CSF. The sub-diploid population was measured by flow cytometry after propidium iodide staining. Results are expressed relative to control cells incubated without CSF, which typically amounted to about 40% of cells. In both panels, results are the means ± SD of pooled data from three independent experiments. None of the differences between wild-type and LOX-1 −/−. macrophages was significant.

ligand specificity that is congruent with the ligand specificity that we observed in SRAI/II-deficient macrophages (12). It has been shown that LOX-1 is expressed in monocyte-derived macrophages (14) and in macrophages in atherosclerotic lesions (7). Furthermore, a recent report indicates that LOX-1 accounts for at least half the uptake of oxLDL in PMA-activated HL-60 macrophages (32). However, in the present studies there was no effect of LOX-1 gene inactivation on oxLDL uptake by BMDM or peritoneal macrophages.

One assumption that is implicit in the interpretation of our results is that there is no compensatory increase in the activity of other scavenger receptors in LOX-1 −/− mice and macrophages that exactly balances the effect of the inactivation of LOX-1 gene. A minor contribution of LOX-1 to oxLDL uptake might be masked if there was a high level of nonsaturable uptake mediated by phagocytosis or pinocytosis. However, we have previously shown that at the relatively low concentration of labeled oxLDL used in the present studies, more than 80% of the uptake and degradation of the labeled oxLDL can be competed by 10-fold excess of unlabeled oxLDL or by polyinosinic acid, indicating that the uptake is mediated by a high-affinity saturable mechanism, presumably a receptor(s) (12, 33). Overall, our finding that LOX-1 gene inactivation does not significantly alter oxLDL uptake in unstimulated murine macrophages indicates that LOX-1 accounts for at most 5–10% of oxLDL uptake by these cells. On the other hand, when LOX-1 was upregulated in macrophages by preincubation with lysophosphatidylcholine, internalization of ox-LDL increased by more than 40%. It has been shown that pro-inflammatory cytokines such as TNFα (34) and TGFβ (35) upregulate LOX-1 and downregulate SR-AI/II and CD36. Hence, it is possible that in microenvironments where these cytokines are relatively abundant, notably in atherosclerotic lesions, LOX-1 might play a significant role in oxLDL uptake. It is also possible that endothelial cells and smooth muscle cells might rely on LOX-1 as a recep-

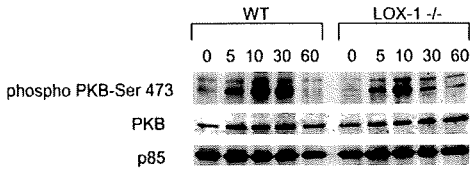

Fig. 8. LOX-1 is not essential for induction of PKB phosphorylation by oxLDL in BMDM. Bone marrow-derived macrophages from wild-type (WT) or LOX-1 knockout mice were incubated with or without 25 μg/ml oxLDL for 0–60 min. Cell lysates were then analyzed by immunoblotting for phosphorylation of PKB at serine 473. Immunostaining for the p85 subunit of PI3K as well as for total PKB was used to monitor loading.

tor for the internalization of oxLDL or for mediating oxLDL-induced signal transduction.

The second issue addressed by these studies was the potential role of LOX-1 in survival signaling. The importance of macrophage survival has been recently underlined by a series of studies in different animal models. Currently it is believed that at least in early stages of atherosclerosis, inhibition of macrophage apoptosis or induction of macrophage growth enhances lesion progression (36). It has been shown that oxLDL activates p42/44 MAPK (15), p38MAPK (37), PKC (38), and PI3K/PKB (15, 26). Activation of PI3K/PKB by oxidized LDL promotes growth and survival of macrophages (15, 26). The upstream steps by which oxLDL activates these signaling pathways have not yet been defined. As LOX-1 has been shown to activate PKCα (39), PKCβ (40), p38MAPK (41), and p42/44MAPK (42), it seemed appropriate to determine if it accounted for part of the anti-apoptotic signaling of oxLDL. However, we found no difference in the anti-apoptotic effect of oxLDL in LOX-1 knockout compared with wild-type macrophages.

In contrast to our findings in BMDM, previous studies in smooth muscle cells (10), cultured endothelial cells (43), and chondrocytes (44) reported a pro-apoptotic effect of oxLDL acting at least in part via LOX-1. There are a number of explanations for these apparently discrepant results. In the study by Kataoka et al. in smooth muscle cells (10), oxLDL only induced apoptosis at concentrations of 40 μg/ml or higher, and Fig. 1A in that paper actually shows increased viability of smooth muscle cells at lower concentrations of oxLDL. Also, they incubated cells in medium containing only 1% fetal bovine serum. We have reported a similar biphasic effect of oxLDL in macrophages, with concentrations higher than 100 μg/ml associated with toxicity in macrophages incubated in 10% fetal bovine serum (15). In macrophages incubated in serum-free medium, the threshold for toxicity of oxLDL was much lower, around 20 μg/ml (15). The study by Imanishi and colleagues found that oxLDL upregulated Fas expression and potentiated the effect of an agonistic anti-Fas antibody on apoptosis in endothelial cells (43). This study did not investigate apoptosis induced by oxLDL, only its effect on apoptosis induced by anti-Fas. In this study, endothelial cells were cultured in medium containing only 1% FBS, which would have made them more vulnerable to toxic effects of oxLDL. The study by Nakagawa and coworkers showed that in chondrocytes, oxLDL at concentrations of 40 μg/ml or higher induced apoptosis. Chondrocytes were incubated in serum-free medium, which may explain why the toxic threshold for oxLDL was relatively low. Also, their oxLDL preparations may not have been dialyzed after oxidation, and we have previously shown that this results in a high concentration of toxic water-soluble aldehydes in the oxLDL mixture (45) Although, it appears that LOX-1 plays a role in oxLDL-mediated toxicity in these cells, our results in macrophages provide no evidence that LOX-1 is involved in the anti-apoptotic effect of low concentrations of oxLDL.

Other receptors that are capable of binding oxLDL or some of its components could play a role in pro-survival signaling, including the phosphatidylserine receptor (46), PPARα (47, 48), PPARγ (49–51), TLR4 (52), and FcγRII (53). Studies are under way to determine if any of these play a role in the pro-survival effect of oxLDL in macrophages.

Dr. Osamu Cynshi provided LOX-1 knockout mice from a colony maintained at Chugai Pharmaceutical Corp., Tokyo.

REFERENCES

1. Moriwaki, H., N. Kume, T. Sawamura, T. Aoyama, H. Hoshikawa, H. Ochi, E. Nishi, T. Masaki, and T. Kita. 1998. Ligand specificity of LOX-1, a novel endothelial receptor for oxidized low density lipoprotein. *Arterioscler. Thromb. Vasc. Biol.* **18:** 1541–1547.
2. Chen, M., T. Masaki, and T. Sawamura. 2002. LOX-1, the receptor for oxidized low-density lipoprotein identified from endothelial cells: implications in endothelial dysfunction and atherosclerosis. *Pharmacol. Ther.* **95:** 89–100.
3. Sawamura, T., N. Kume, T. Aoyama, H. Moriwaki, H. Hoshikawa, Y. Aiba, T. Tanaka, S. Miwa, Y. Katsura, T. Kita, et al. 1997. An endothelial receptor for oxidized low-density lipoprotein. *Nature.* **386:** 73–77.
4. Cominacini, L., A. F. Pasini, U. Garbin, A. Davoli, M. L. Tosetti, M. Campagnola, A. Rigoni, A. M. Pastorino, V. Lo Cascio, and T. Sawamura. 2000. Oxidized low density lipoprotein (ox-LDL) binding to ox-LDL receptor-1 in endothelial cells induces the activation of NF-kappaB through an increased production of intracellular reactive oxygen species. *J. Biol. Chem.* **275:** 12633–12638.
5. Cominacini, L., A. Rigoni, A. F. Pasini, U. Garbin, A. Davoli, M. Campagnola, A. M. Pastorino, V. Lo Cascio, and T. Sawamura. 2001. The binding of oxidized low density lipoprotein (ox-LDL) to ox-LDL receptor-1 reduces the intracellular concentration of nitric oxide in endothelial cells through an increased production of superoxide. *J. Biol. Chem.* **276:** 13750–13755.
6. Li, D., and J. Mehta. 2000. Upregulation of endothelial receptor for oxidized LDL (LOX-1) by oxidized LDL and implications in apoptosis of human coronary artery endothelial cells. Evidence from use of antisense LOX-1 mRNA and chemical inhibitors. *Arterioscler. Thromb. Vasc. Biol.* **20:** 1116–1122.
7. Kataoka, H., N. Kume, S. Miyamoto, M. Minami, H. Moriwaki, T. Murase, T. Sawamura, T. Masaki, N. Hashimoto, and T. Kita. 1999. Expression of lectinlike oxidized low-density lipoprotein receptor-1 in human atherosclerotic lesions. *Circulation.* **99:** 3110–3117.
8. Chen, C. H., W. Jiang, D. P. Via, S. Luo, T. R. Li, Y. T. Lee, and P. D. Henry. 2000. Oxidized low-density lipoproteins inhibit endothelial cell proliferation by suppressing basic fibroblast growth factor expression. *Circulation.* **101:** 171–177.
9. Mehta, J. L., N. Sanada, C. P. Hu, J. Chen, A. Dandapat, F. Sugawara, H. Satoh, K. Inoue, Y. Kawase, K. Jishage, et al. 2007. Deletion of LOX-1 reduces atherogenesis in LDLR knockout mice fed high cholesterol diet. *Circ. Res.* **100:** 1634–1642.

10. Kataoka, H., N. Kume, S. Miyamoto, M. Minami, M. Morimoto, K. Hayashida, N. Hashimoto, and T. Kita. 2001. Oxidized LDL modulates Bax/Bcl-2 through the lectinlike Ox-LDL receptor-1 in vascular smooth muscle cells. *Arterioscler. Thromb. Vasc. Biol.* **21:** 955–960.
11. Greaves, D. R., and S. Gordon. 2005. Thematic review series: The immune system and atherogenesis. Recent insights into the biology of macrophage scavenger receptors. *J. Lipid Res.* **46:** 11–20.
12. Lougheed, M., C. Ming Lum, W. Ling, H. Suzuki, T. Kodama, and U. P. Steinbrecher. 1997. High-affinity saturable uptake of oxidized low density lipoprotein by macrophages from mice lacking the scavenger receptor class A type I/II. *J. Biol. Chem.* **272:** 12938–12944.
13. Kunjathoor, V. V., M. Febbraio, E. A. Podrez, K. J. Moore, L. Andersson, S. Koehn, J. S. Rhee, R. Silverstein, H. F. Hoff, and M. W. Freeman. 2002. Scavenger receptors class A-I/II and CD36 are the principal receptors responsible for the uptake of modified low density lipoprotein leading to lipid loading in macrophages. *J. Biol. Chem.* **277:** 49982–49988.
14. Yoshida, H., N. Kondratenko, S. Green, D. Steinberg, and O. Quehenberger. 1998. Identification of the lectin-like receptor for oxidized low-density lipoprotein in human macrophages and its potential role as a scavenger receptor. *Biochem. J.* **334:** 9–13.
15. Hundal, R., B. Salh, J. Schrader, A. Gómez-Muñoz, V. Duronio, and U. Steinbrecher. 2001. Oxidized low density lipoprotein inhibits macrophage apoptosis through activation of the PI 3-kinase/PKB pathway. *J. Lipid Res.* **42:** 1483–1491.
16. Hundal, R., A. Gómez-Muñoz, J. Kong, B. Salh, A. Marotta, V. Duronio, and U. Steinbrecher. 2003. Oxidized low density lipoprotein inhibits macrophage apoptosis by blocking ceramide generation, thereby maintaining PKB activation and Bcl-XL levels. *J. Biol. Chem.* **278:** 24399–24408.
17. Martens, J., M. Lougheed, A. Gomez-Muñoz, and U. Steinbrecher. 1999. A modification of apolipoprotein B accounts for most of the induction of macrophage growth by oxidized low density lipoprotein. *J. Biol. Chem.* **274:** 10903–10910.
18. Matsunaga, T., S. Hokari, I. Koyama, T. Harada, and T. Komoda. 2003. NF-kappa B activation in endothelial cells treated with oxidized high-density lipoprotein. *Biochem. Biophys. Res. Commun.* **303:** 313–319.
19. Havel, R. J., H. A. Eder, and J. H. Bragdon. 1955. The distribution and chemical composition of ultracentrifugally separated lipoproteins in human serum. *J. Clin. Invest.* **43:** 1345–1353.
20. Bilheimer, D. W., S. Eisenberg, and R. I. Levy. 1972. The metabolism of very low density lipoproteins. *Biochim. Biophys. Acta.* **260:** 212–221.
21. Steinbrecher, U. P. 1987. Oxidation of human low density lipoproteins results in derivatization of lysine residues of apolipoprotein B by lipid peroxide decomposition products. *J. Biol. Chem.* **262:** 3603–3608.
22. Zhang, H., Y. Yang, and U. P. Steinbrecher. 1993. Structural requirements for the binding of modified proteins to the scavenger receptor of macrophages. *J. Biol. Chem.* **268:** 5535–5542.
23. Hamilton, J. A., D. Myers, W. Jessup, F. Cochrane, R. Byrne, G. Whitty, and S. Moss. 1999. Oxidized LDL can induce macrophage survival, DNA synthesis, and enhanced proliferative response to CSF-1 and GM-CSF. *Arterioscler. Thromb. Vasc. Biol.* **19:** 98–105.
24. Pitas, R. E., T. L. Innerarity, J. N. Weinstein, and R. W. Mahley. 1981. Acetoacetylated lipoproteins used to distinguish fibroblasts from macrophages in vitro by fluorescence microscopy. *Arteriosclerosis.* **1:** 177–185.
25. Ling, W., M. Lougheed, H. Suzuki, A. Buchan, T. Kodama, and U. Steinbrecher. 1997. Oxidized or acetylated low density lipoprotein are rapidly cleared by the liver in mice with disruption of the scavenger receptor class A type I/type II gene. *J. Clin. Invest.* **100:** 244–252.
26. Martens, J., N. Reiner, P. Herrera-Velit, and U. Steinbrecher. 1998. Phosphatidylinositol 3-kinase is involved in the induction of macrophage growth by oxidized low density lipoprotein. *J. Biol. Chem.* **273:** 4915–4920.
27. Lowry, O. H., N. J. Rosebrough, A. L. Farr, and R. J. Randall. 1951. Protein measurement with the Folin phenol reagent. *J. Biol. Chem.* **193:** 265–275.
28. Stephan, Z., and E. Yurachek. 1993. Rapid fluorometric assay of LDL receptor activity by DiI-labelled LDL. *J. Lipid Res.* **34:** 325–330.
29. Aoyama, T., H. Fujiwara, T. Masaki, and T. Sawamura. 1999. Induction of lectin-like oxidized LDL receptor by oxidized LDL and lysophosphatidylcholine in cultured endothelial cells. *J. Mol. Cell. Cardiol.* **31:** 2101–2114.
30. Aoyama, T., M. Chen, H. Fujiwara, T. Masaki, and T. Sawamura. 2000. LOX-1 mediates lysophosphatidylcholine-induced oxidized LDL uptake in smooth muscle cells. *FEBS Lett.* **467:** 217–220.
31. Kakutani, M., M. Ueda, T. Naruko, T. Masaki, and T. Sawamura. 2001. Accumulation of LOX-1 ligand in plasma and atherosclerotic lesions of Watanabe heritable hyperlipidemic rabbits: identification by a novel enzyme immunoassay. *Biochem. Biophys. Res. Commun.* **282:** 180–185.
32. Smirnova, I. V., M. Kajstura, T. Sawamura, and M. S. Goligorsky. 2004. Asymmetric dimethylarginine upregulates LOX-1 in activated macrophages: role in foam cell formation. *Am. J. Physiol. Heart Circ. Physiol.* **287:** H782–H790.
33. Lougheed, M., and U. P. Steinbrecher. 1996. Mechanism of uptake of copper-oxidized low density lipoprotein in macrophages is dependent on its extent of oxidation. *J. Biol. Chem.* **271:** 11798–11805.
34. Kume, N., H. Moriwaki, H. Kataoka, M. Minami, T. Murase, T. Sawamura, T. Masaki, and T. Kita. 2000. Inducible expression of LOX-1, a novel receptor for oxidized LDL, in macrophages and vascular smooth muscle cells. *Ann. N. Y. Acad. Sci.* **902:** 323–327.
35. Draude, G., and R. L. Lorenz. 2000. TGF-beta1 downregulates CD36 and scavenger receptor A but upregulates LOX-1 in human macrophages. *Am. J. Physiol. Heart Circ. Physiol.* **278:** H1042–H1048.
36. Tabas, I. 2005. Consequences and therapeutic implications of macrophage apoptosis in atherosclerosis: the importance of lesion stage and phagocytic efficiency. *Arterioscler. Thromb. Vasc. Biol.* **25:** 2255–2264.
37. Salomonsson, L., S. Pettersson, M. C. Englund, O. Wiklund, and B. G. Ohlsson. 2002. Post-transcriptional regulation of VEGF expression by oxidised LDL in human macrophages. *Eur. J. Clin. Invest.* **32:** 767–774.
38. Claus, R., B. Fyrnys, H. P. Deigner, and G. Wolf. 1996. Oxidized low-density lipoprotein stimulates protein kinase C (PKC) and induces expression of PKC-isotypes via prostaglandin-H-synthase in P388D1 macrophage-like cells. *Biochemistry.* **35:** 4911–4922.
39. Li, D., L. Liu, H. Chen, T. Sawamura, and J. L. Mehta. 2003. LOX-1, an oxidized LDL endothelial receptor, induces CD40/CD40L signaling in human coronary artery endothelial cells. *Arterioscler. Thromb. Vasc. Biol.* **23:** 816–821.
40. Li, D., L. Liu, H. Chen, T. Sawamura, S. Ranganathan, and J. L. Mehta. 2003. LOX-1 mediates oxidized low-density lipoprotein-induced expression of matrix metalloproteinases in human coronary artery endothelial cells. *Circulation.* **107:** 612–617.
41. Iwai-Kanai, E., K. Hasegawa, T. Sawamura, M. Fujita, T. Yanazume, S. Toyokuni, S. Adachi, Y. Kihara, and S. Sasayama. 2001. Activation of lectin-like oxidized low-density lipoprotein receptor-1 induces apoptosis in cultured neonatal rat cardiac myocytes. *Circulation.* **104:** 2948–2954.
42. Li, D., and J. L. Mehta. 2000. Antisense to LOX-1 inhibits oxidized LDL-mediated upregulation of monocyte chemoattractant protein-1 and monocyte adhesion to human coronary artery endothelial cells. *Circulation.* **101:** 2889–2895.
43. Imanishi, T., T. Hano, T. Sawamura, S. Takarada, and I. Nishio. 2002. Oxidized low density lipoprotein potentiation of Fas-induced apoptosis through lectin-like oxidized-low density lipoprotein receptor-1 in human umbilical vascular endothelial cells. *Circ. J.* **66:** 1060–1064.
44. Nakagawa, T., T. Yasuda, H. Hoshikawa, M. Shimizu, T. Kakinuma, M. Chen, T. Masaki, T. Nakamura, and T. Sawamura. 2002. LOX-1 expressed in cultured rat chondrocytes mediates oxidized LDL-induced cell death-possible role of dephosphorylation of Akt. *Biochem. Biophys. Res. Commun.* **299:** 91–97.
45. Steinbrecher, U. P., A. Gomez-Munoz, and V. Duronio. 2004. Acid sphingomyelinase in macrophage apoptosis. *Curr. Opin. Lipidol.* **15:** 531–537.
46. Fadok, V. A., D. Xue, and P. Henson. 2001. If phosphatidylserine is the death knell, a new phosphatidylserine-specific receptor is the bellringer. *Cell Death Differ.* **8:** 582–587.
47. Delerive, P., C. Furman, E. Teissier, J. Fruchart, P. Duriez, and B. Staels. 2000. Oxidized phospholipids activate PPARalpha in a phospholipase A2-dependent manner. *FEBS Lett.* **471:** 34–38.
48. Lee, H., W. Shi, P. Tontonoz, S. Wang, G. Subbanagounder, C. C. Hedrick, S. Hama, C. Borromeo, R. M. Evans, J. A. Berliner, et al. 2000. Role for peroxisome proliferator-activated receptor alpha in oxidized phospholipid-induced synthesis of monocyte chemotac-

tic protein-1 and interleukin-8 by endothelial cells. *Circ. Res.* **87:** 516–521.
49. Nagy, L., P. Tontonoz, J. Alvarez, H. Chen, and R. Evans. 1998. Oxidized LDL regulates macrophage gene expression through ligand activation of PPARg. *Cell.* **93:** 229–240.
50. Davies, S. S., A. V. Pontsler, G. K. Marathe, K. A. Harrison, R. C. Murphy, J. C. Hinshaw, G. D. Prestwich, A. S. Hilaire, S. M. Prescott, G. A. Zimmerman, et al. 2001. Oxidized alkyl phospholipids are specific, high affinity peroxisome proliferator-activated receptor gamma ligands and agonists. *J. Biol. Chem.* **276:** 16015–16023.
51. Pontsler, A. V., A. St Hilaire, G. K. Marathe, G. A. Zimmerman, and T. M. McIntyre. 2002. Cyclooxygenase-2 is induced in monocytes by peroxisome proliferator activated receptor gamma and oxidized alkyl phospholipids from oxidized low density lipoprotein. *J. Biol. Chem.* **277:** 13029–13036.
52. Miller, Y. I., S. Viriyakosol, C. J. Binder, J. R. Feramisco, T. N. Kirkland, and J. L. Witztum. 2003. Minimally modified LDL binds to CD14, induces macrophage spreading via TLR4/MD-2, and inhibits phagocytosis of apoptotic cells. *J. Biol. Chem.* **278:** 1561–1568.
53. Stanton, L. W., R. T. White, C. M. Bryant, A. A. Protter, and G. Endemann. 1992. A macrophage Fc receptor for IgG is also a receptor for oxidized low density lipoprotein. *J. Biol. Chem.* **267:** 22446–22451.

Cardiovascular Research (2009) 84, 127–136
doi:10.1093/cvr/cvp177

LOX-1-MT1-MMP axis is crucial for RhoA and Rac1 activation induced by oxidized low-density lipoprotein in endothelial cells

Koichi Sugimoto[1], Toshiyuki Ishibashi[1]*, Tatsuya Sawamura[2,3], Nobutaka Inoue[2], Masashi Kamioka[1], Hironori Uekita[1], Hiroshi Ohkawara[1], Takayuki Sakamoto[1], Nobuo Sakamoto[1], Yasuo Okamoto[4], Yoh Takuwa[4], Akemi Kakino[2], Yoshiko Fujita[2], Takeshi Tanaka[3], Tamio Teramoto[5], Yukio Maruyama[1,6], and Yasuchika Takeishi[1]

[1]*First Department of Internal Medicine, Fukushima Medical University, 1 Hikarigaoka, Fukushima 960-1295, Japan;* [2]*Department of Bioscience, National Cardiovascular Center Research Institute, Osaka, Japan;* [3]*International Research and Educational Institute for Integrated Medical Sciences, Tokyo Women's University, Tokyo, Japan;* [4]*Department of Physiology, Kanazawa University Graduate School of Medicine, Kanazawa, Japan;* [5]*Department of Internal Medicine, Teikyo University School of Medicine, Tokyo, Japan; and* [6]*Hoshi General Hospital, Fukushima, Japan*

Received 14 October 2008; revised 8 May 2009; accepted 26 May 2009; online publish-ahead-of-print 1 June 2009

Time for primary review: 25 days

KEYWORDS
LOX-1;
MT1-MMP;
RhoA;
Rac1;
Endothelial dysfunction

Aims RhoA and Rac1 activation plays a key role in endothelial dysfunction. Lectin-like oxidized low-density lipoprotein receptor-1 (LOX-1) is a major receptor for oxidized low-density lipoprotein (ox-LDL) in endothelial cells (ECs). Membrane type 1 matrix metalloproteinase (MT1-MMP) has been shown to be involved in atherogenesis. This study was conducted to investigate the role of the LOX-1-MT1-MMP axis in RhoA and Rac1 activation in response to ox-LDL in ECs.

Methods and results Ox-LDL induced rapid RhoA and Rac1 activation as well as MT1-MMP activity in cultured human aortic ECs. Inhibition of LOX-1 prevented ox-LDL-dependent RhoA and Rac1 activation. Knockdown of MT1-MMP by small interfering RNA prevented ox-LDL-induced RhoA and Rac1 activation, indicating that MT1-MMP is upstream of RhoA and Rac1. Fluorescent immunostaining revealed the colocalization of LOX-1 and MT1-MMP, and the formation of a complex of LOX-1 with MT1-MMP was detected by immunoprecipitation. Blockade of LOX-1 or MT1-MMP prevented RhoA-dependent endothelial NO synthase protein downregulation and cell invasion, Rac1-mediated NADPH oxidase activity, and reactive oxygen species generation.

Conclusion The present study provides evidence that the LOX-1-MT1-MMP axis plays a crucial role in RhoA and Rac1 activation signalling pathways in ox-LDL stimulation, suggesting that this axis may be a promising target for treating endothelial dysfunction.

1. Introduction

Endothelial dysfunction is crucial for the initiation and development of atherosclerosis.[1,2] Oxidized low-density lipoprotein (ox-LDL) impairs endothelial function, giving rise to reactive oxygen species (ROS) generation, and reduced nitric oxide (NO) production.[1,2] It is widely acknowledged that ox-LDL downregulates the expression of endothelial nitric oxide synthase (eNOS), which is associated with the activation of small GTP-binding protein, RhoA.[3] Earlier, we reported that lysophosphatidylcholine, a phospholipid compound of ox-LDL, activates RhoA within 1 min in cultured human aortic endothelial cells (HAECs).[4] These observations indicate that rapid RhoA activation plays a pivotal role in the downregulation of eNOS induced by ox-LDL. Ox-LDL-triggered ROS generation is predominantly mediated via NADPH oxidase in the vasculature, and small GTP-binding protein Rac1 is a component of NADPH oxidase,[2,5–7] indicating that Rac1 is critical for ox-LDL-stimulated ROS generation via NADPH oxidase in ECs. Lectin-like ox-LDL receptor-1 (LOX-1) with a type II membrane protein structure has been identified as a major endothelial receptor for ox-LDL in endothelial cells (ECs).[8] Thus, an ox-LDL-LOX-1 axis appears to be crucial for the pathogenesis of endothelial dysfunction in coronary artery disease. However, there is no report indicating that LOX-1 forms a complex with other molecule(s).

Degradation of the vascular extracellular matrix by secreted and membrane type matrix metalloproteinases

* Corresponding author. Tel: +81 24 547 1190; fax: +81 24 548 1821.
E-mail address: masaishi@fmu.ac.jp

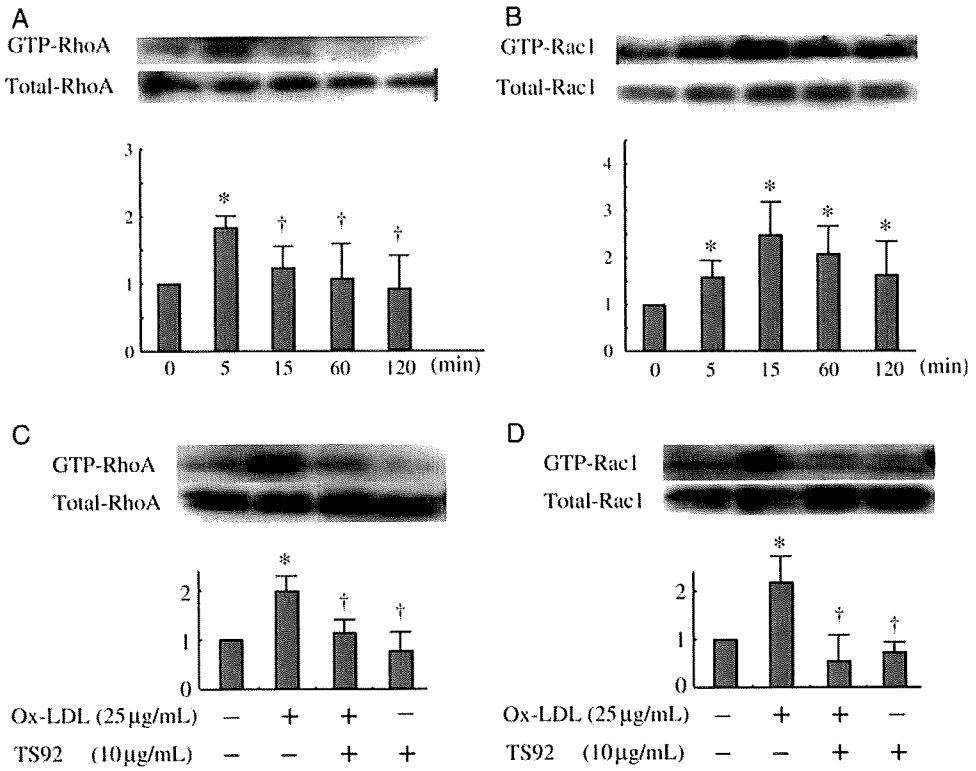

Figure 1 Role of LOX-1 in ox-LDL-triggered RhoA and Rac1 activation. (*A*, *B*) Levels of GTP-bound active forms of RhoA and Rac1 as determined by pull-down assays in cultured human aortic endothelial cells (HAECs) 5–120 min after adding 25 μg/mL ox-LDL. (*C*, *D*) Effects of inhibition of LOX-1 on ox-LDL-induced GTP/GDP exchange (GTP-loading) of RhoA and Rac1. TS92 (10 μg/mL), a monoclonal antibody to LOX-1, was added to HAECs 60 min before adding ox-LDL. The GTP-loading of RhoA and Rac1 was determined by pull-down assays after 5 and 15 min of ox-LDL stimulation, respectively. Quantitative results of GTP-RhoA and GTP-Rac1 were normalized by total RhoA or Rac1 levels. Bars are mean ± SD of quantitative densitometric analyses from three separate experiments. Representative immunoblots are shown at the top. $^{*}P < 0.05$ vs. control; $^{\dagger}P < 0.05$ vs. ox-LDL.

(secreted MMPs and MT-MMPs) plays an important role in smooth muscle cell migration and invasion and plaque instability, which in turn, contribute to the pathogenesis of coronary artery disease, especially acute coronary syndromes.[9] Ox-LDL has been shown to increase the expression and activities of MMPs including secreted MMPs and MT-MMPs.[10,11] MT-MMPs possess transmembrane and cytoplasmic domains in addition to extracellular domains. The activities of secreted MMPs and MT-MMPs are modulated by the tissue inhibitor of metalloproteinases (TIMPs). MT-MMPs are inhibited by TIMP-2, whereas TIMP-1 and TIMP-2 inhibit secreted MMPs. Membrane type 1 MMP (MT1-MMP) participates in skeletal development, cell growth, and angiogenesis.[12,13] MT1-MMP also has been shown to play a role in cell migration and invasion mediated via the Rho family of GTPases such as Rho, Rac, and Cdc42.[14–16]

In the present study, we hypothesized that MT1-MMP plays an integral role in ox-LDL-triggered RhoA and Rac1 signalling pathways and that MT1-MMP and LOX-1 may form a complex.

2. Methods

The investigation conforms with the principles outlined in the Declaration of Helsinki.[17]

2.1 Materials

The sources of most of the conventional reagents were described previously.[18,19] Recombinant human TIMP-1 and TIMP-2 were obtained from DAIICHI Fine Chemical Co., Ltd (Toyama, Japan). Neutralizing antibody to LOX-1, TS92, was used for the inhibition of LOX-1.[10] Diphenyleneiodonium (DPI), a selective NADPH oxidase inhibitor, was from Sigma-Aldrich Co. (St Louis, MO, USA) and C3 exoenzyme, a Rho inhibitor, from Upstate Biotechnology (Lake Placid, NY, USA).

2.2 Preparation of ECs

HAECs were cultured according to the suppliers' instructions (Clonetics Inc., Walkersville, MD, USA and Sanko Junyaku Co., Ltd, Tokyo, Japan) and used for all experiments after 5–10 passages.[4,20]

2.3 Preparation of ox-LDL

Human LDL was isolated from the serum of fasting normolipidaemic volunteers by sequential ultracentrifugation and ox-LDL was prepared by incubating native LDL for 24 h at 4°C in phosphate-buffered saline (PBS) containing 5 μmol/L $CuSO_4$, and then extensively dialyzed against PBS and sterilized by filtration as described previously.[21]

2.4 Western blotting

The expression of RhoA, Rac1, eNOS, and α-tubulin was determined by western blotting.[4,20,22] For immunoblotting, we used mouse monoclonal antibodies to RhoA (Santa Cruz Biotechnology, Santa Cruz, CA, USA) and Rac1 (Upstate Biotechnology) diluted 1:500, and to eNOS (Transduction Laboratories, Lexington, KY, USA) diluted 1:1000 and α-tubulin (Santa Cruz Biotechnology) diluted 1:500. The signals from immunoreactive bands were visualized by

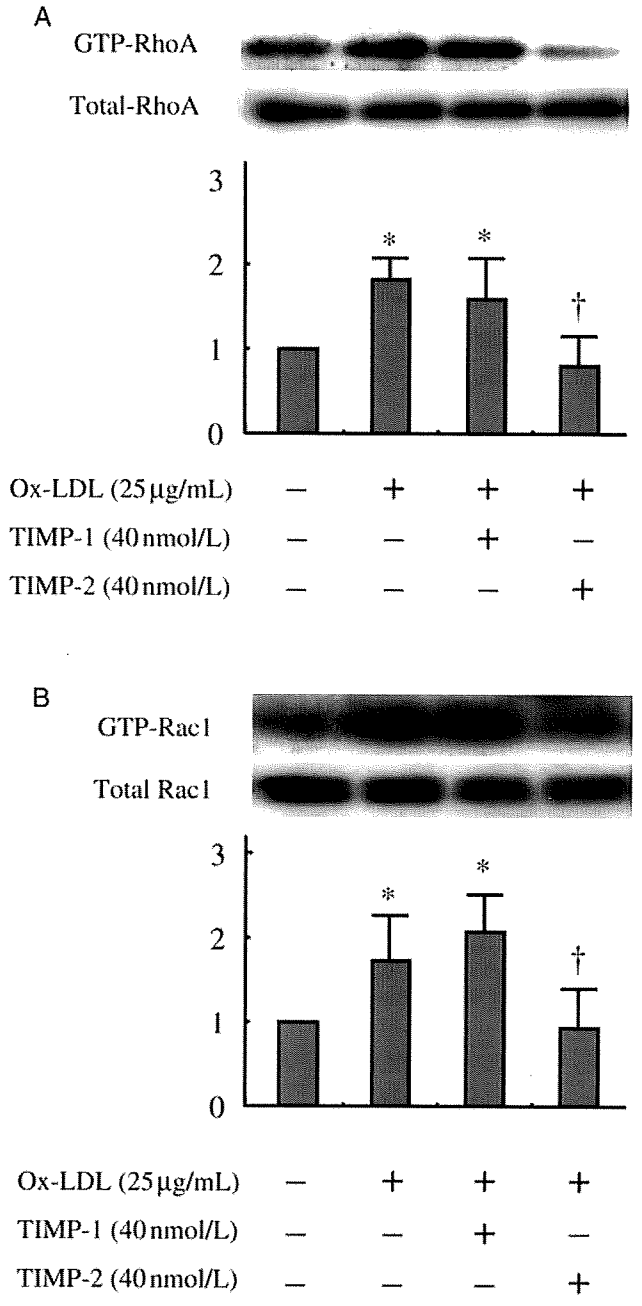

Figure 2 Effects of TIMP-1 and TIMP-2 on ox-LDL-triggered GTP-loading of RhoA (*A*) and Rac1 (*B*). HAECs were pretreated with 40 nmol/L TIMP-1 or TIMP-2 for 60 min before adding ox-LDL. After 5 and 15 min of ox-LDL stimulation, the GTP-loading of RhoA and Rac1 was determined. TIMP indicates tissue inhibitor of metalloproteinase. Bars are mean ± SD of quantitative densitometric analyses from three separate experiments. Representative immunoblots are shown at the top. $^{*}P < 0.05$ vs. control; $^{\dagger}P < 0.05$ vs. ox-LDL.

an Amersham ECL system (Amersham Pharmacia Biotech UK Ltd, Buckinghamshire, UK).

2.5 GTP/GDP exchange of RhoA and Rac1

GTP-bound active forms of RhoA and Rac1 were determined by pull-down assay as described previously.[4,20,22] Extracts of HAECs were incubated at 4°C for 45 min with glutathione-Sepharose 4B beads coupled with glutathione-S-transferase (GST)-rhotekin fusion protein for determination of RhoA activity or GST-p21-activated

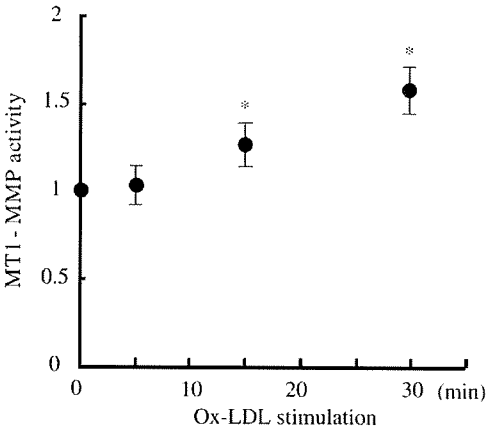

Figure 3 Plasma membrane fractions were extracted from HAECs at the time indicated after ox-LDL stimulation, and thereafter the activity of MT1-MMP was determined as described in the Methods section. Results are expressed as mean ± SD of three separate experiments performed in pentaplicate. $^{*}P < 0.05$ vs. control.

kinase for determination of Rac1 activity. Bound RhoA and Rac1 were semi-quantitatively detected by western blotting.

2.6 Measurement of MT1-MMP activity of membrane fractions

To evaluate MT1-MMP activity, we prepared membrane fractions of HAECs as described previously.[4,21] Briefly, cells were lysed with a hypotonic buffer, then sonicated and centrifuged at 15 000 *g* for 10 min. The separated membrane fractions were assessed by the commercially available fluorescent assay kit (SensoLyte 520 MMP-14 assay kit, AnaSpec, San Jose, CA, USA) according to the manufacturer's instructions.

2.7 Small interfering RNA

MT1-MMP expression was silenced by siRNA 5′-CUGGCAGUUCGGC UAGAUUUC-3′ (sense strand for MT1-MMP) (RNAi Co., Ltd, Tokyo, Japan).[23] HAECs were transfected with double-strand siRNA in serum-free medium mixed with oligofectamine (Invitrogen, Carlsbad, CA, USA) according to the manufacturer's instructions. Four hours after transfection, HAECs were incubated in a medium containing 2% foetal bovine serum (FBS) for 48 h. Alternatively, cells were treated with an irrelevant siRNA 5′-GUACCGCACGUCA UUCGCAUC-3′ (sense strand) as a negative control.

2.8 Generation of anti-human LOX-1 monoclonal antibodies

Anti-human LOX-1 monoclonal antibodies were generated by immunizing Balb/c mice subcutaneously with the recombinant protein of the extracellular domain of LOX-1, LOX-1(61–273).[24] The splenocytes from the immunized mice were fused with myeloma cell line, P3U1, and the resultant hybridomas were screened using enzyme-linked immunosorbent assay to the antigen. Among the positive clones, purified monoclonal antibody from clone #1-1 was used for western blotting, and another antibody from #10-1 was used for immunocytochemistry.

2.9 Fluorescent immunostaining

A mouse monoclonal antibody available to LOX-1 (termed #10-1) was used for immunostaining.[8] HAECs cultured on chamber slides were fixed in 10% formalin for 10 min, and then incubated with the antibodies to LOX-1 and MT1-MMP (Chemicon International, Inc., Temecula, CA, USA) at room temperature for 60 min. After washing, anti-mouse Alexa 488 and anti-rabbit Alexa 594 (Molecular

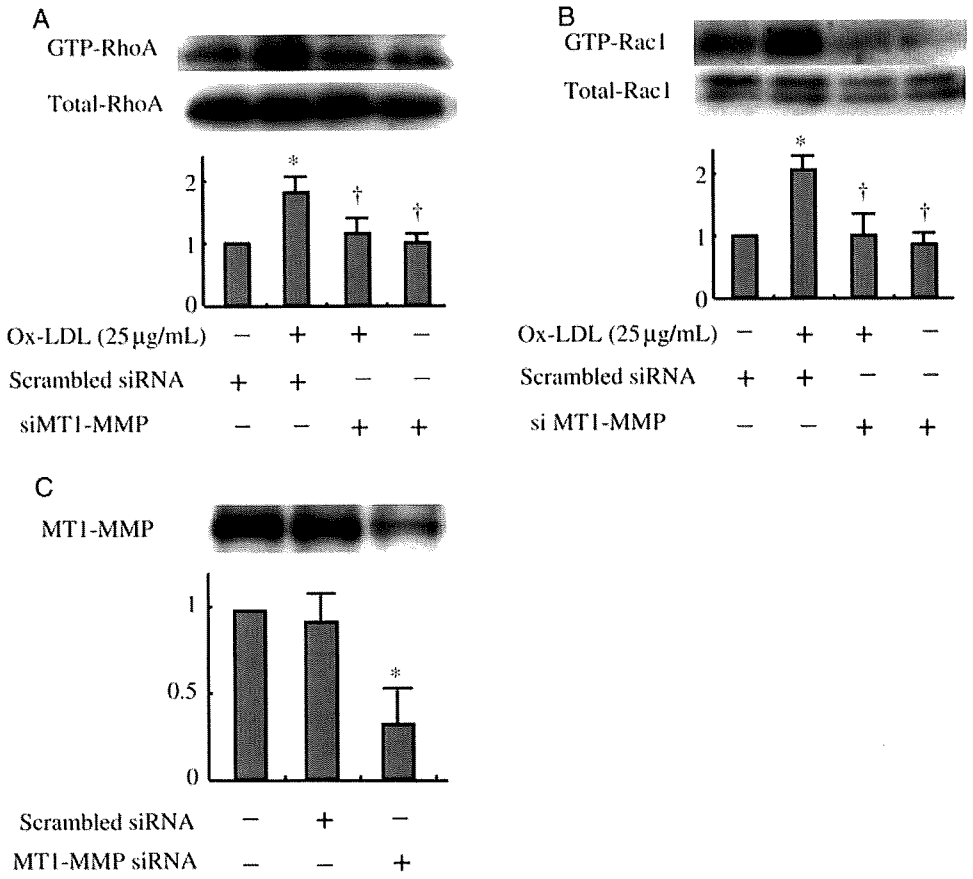

Figure 4 Role of MT1-MMP in ox-LDL-triggered RhoA and Rac1 activation. (*A*, *B*) Effect of knockdown of MT1-MMP by siRNA on increased GTP-loading of RhoA and Rac1 caused by ox-LDL. Cells were incubated in the presence of 25 μg/mL ox-LDL after transfection of MT1-MMP siRNA or scrambled siRNA. The amounts of the GTP-bound forms of RhoA and Rac1 were determined by western blotting. Bars are mean ± SD of four separate experiments. Representative immunoblots from four separate experiments are shown. *$P < 0.05$ vs. control; †$P < 0.05$ vs. ox-LDL. (*C*) Effect of knockdown of MT1-MMP by siRNA on the MT1-MMP protein level as determined by western blotting. Bars are mean ± SD of three separate experiments. Representative immunoblots from three independent experiments are shown. *$P < 0.05$ vs. control.

Probes, Eugene, OR, USA) were reacted for 60 min. Stained cells were stored in the dark until they were analyzed by a confocal microscope (Olympus, Tokyo, Japan).

2.10 Immunoprecipitation

HAECs were extracted in a RIPA buffer (Sigma–Aldrich), and the lysates were centrifuged at 10 000 *g* at 4°C. The supernatant was precleared and reacted with anti-MT1-MMP (Chemicon) and anti-LOX-1 antibody (R&D Systems Inc., Minneapolis, MN, USA) at a concentration of 1.0 μg/mL, respectively. Immunoprecipitated protein was resolved by sodium dodecyl sulfate–polyacrylamide gel electrophoresis, followed by western blotting of LOX-1 and MT1-MMP, respectively. The positive controls of endothelial cell lysate were loaded. We used the primary antibody against LOX-1 (termed #1-1) and MT1-MMP (Chemicon), and anti-mouse or anti-rabbit IgG True blot™ (eBioscience, Inc., San Diego, CA, USA), which detects native antibody but not the denatured 55 kDa heavy chain and 23 kDa light chains of the immunoprecipitating antibody, as the secondary antibody.

2.11 Adenovirus gene transfer

HAECs were infected with adenoviruses encoding a dominant negative form of N19RhoA, N17Rac or *LacZ* at a multiplicity of infection of approximately 50 as described previously.[22,25] This procedure resulted in the expression of *LacZ* as a marker gene in nearly 100% of the transfected cells. After transfection, cells were washed three times with PBS and incubated for 48 h in medium containing 2% FBS, followed by the experiments.

2.12 EC invasion assay

EC invasion was assayed by a commercially available kit (BD Biocoat™ Angiogenesis System: Endothelial Cell Invasion, BD Biosciences, Bedford, MA, USA) according to the manufacturer's instructions. Briefly, HAECs were pretreated with N19RhoA or MT1-MMP siRNA as described above and then stimulated with 25 μg/mL ox-LDL for 12 h. Invasive cells were fluorescently labelled with Calcein-AM and the fluorescence intensity was quantitatively determined by Image J 1.34 (National Institutes of Health, Bethesda, MD, USA).

2.13 Measurement of intracellular ROS generation

Detection of intracellular ROS generation was performed by a previously established method using the ROS-sensitive fluorescent probe 2′,7′-dichlorodihydro-fluorescein-diacetate (H_2DCF-DA) (Molecular Probes).[5] HAECs were incubated in 2% FBS-containing medium and 10 μmol/L H_2DCF-DA for 10 min. Ox-LDL (25 μg/mL) was added to the cells and incubated for up to 60 min at 37°C. The fluorescence was measured using a fluorescent microscope (Olympus) at an excitation and emission wavelength of 475 nm and 525 nm, respectively. DCF fluorescence intensity was quantitatively determined by Image J 1.34. For each photograph, the cellular and background fluorescence values were obtained by tracing the

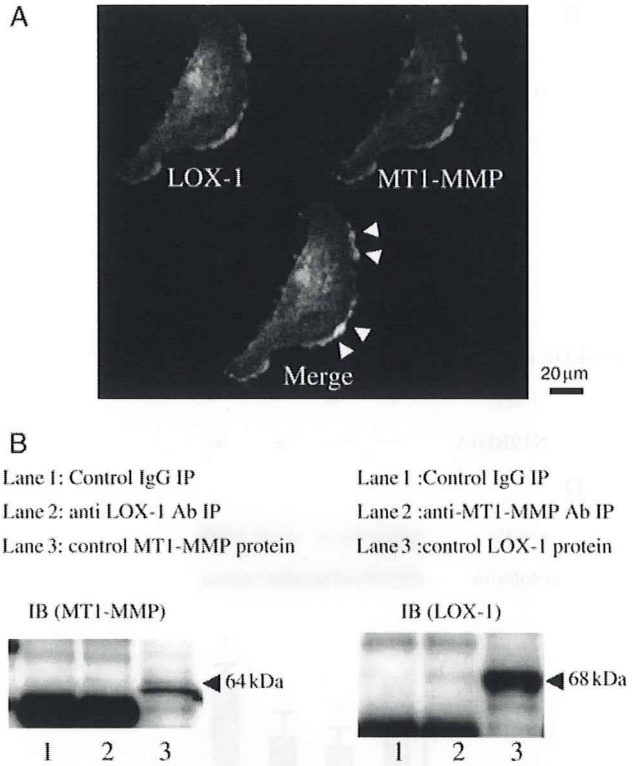

Figure 5 (*A*) Association of LOX-1 and MT1-MMP according to fluorescent immunohistochemistry. Merged image indicates that LOX-1 is partially colocalized with MT1-MMP. Photomicrographs are from an experiment representative of 10 independent experiments. (*B*) Formation of a complex of LOX-1 and MT1-MMP as determined by immunoprecipitation. In the left panel, 64 kDa band recognized by immunoblotting with anti-MT1-MMP antibody was detected in the LOX-1-immunoprecipitates (lane 2). Immunoprecipitates made using an isotype-matched control antibody did not show 64-kDa band (left panel, lane 1), whereas 64 kDa band was recognized in control cell lysate. In a reversed experiment, LOX-1 (70 kDa) was detected from MT1-MMP immunoprecipitates (right panel, lane 2), whereas control antibody-associated immunoprecipitates did not contain the LOX-1 band (right panel, lane 1). Each control immunoblot of endothelial cell lysate is shown in lane 3.

shape of cells. Results were displayed in a ratiometric fashion normalized for the control condition.

2.14 Measurement of NADPH oxidase activity

Since ox-LDL increases NADPH oxidase activity, the enzymatic activities of NADPH oxidase of homogenates of the cells were assessed by lucigenin-enhanced chemiluminescence (L-CL) as previously described.[26] The assay solution contained 50 mmol/L HEPES (pH 7.4), 1.0 mmol/L EDTA, 6.5 mmol/L $MgCl_2$, 5.0 μmol/L lucigenin as an electron acceptor and 1 mmol/L NADPH as a substrate. After preincubation at 37°C for 10 min, the reaction was started by adding 50 μg of homogenate. Final volume of the reaction solution was 1.0 mL. Photon emission was continuously recorded for 15 min with a CL reader (ALOKA, BLR-201, Tokyo, Japan). The chemiluminescent signals observed in the absence of homogenates were subtracted from the chemiluminescence signals of the samples. The chemiluminescence signal was corrected for the protein concentration of each cell homogenate and expressed as counts per minute (cpm) per milligram protein for a 15-min period. In some experiments, the homogenates were preincubated with 10 μmol/L DPI for 20 min before L-CL measurement.

2.15 Densitometric analysis and statistical analyses

After scanning blots into a computer (EPSON GT5500ART, Tokyo, Japan), the optical densities of individual immunoblots were analyzed using the NIH IMAGE Program software as described previously.[18,20] Statistical analyses were performed using ANOVA with Scheffé's *post hoc* test if appropriate. A value of $P < 0.05$ was considered significant.

3. Results

3.1 Role of LOX-1 in ox-LDL-induced RhoA and Rac1 signalling

We determined the effect of ox-LDL on RhoA and Rac1 activation in cultured HAECs. Pull-down assays revealed the time-course of GTP-loading of RhoA and Rac1 in response to 25 μg/mL ox-LDL in HAECs (*Figure 1A* and *B*). Ox-LDL increased the GTP-loading of RhoA within 5 min after adding ox-LDL and returned to control after 15 min of ox-LDL stimulation. The GTP-loading of Rac1 was induced 5 min and peaked 15 min after exposure to ox-LDL. The relatively high levels of GTP-loading of Rac1 persisted for at least up to 120 min after ox-LDL stimulation. Next, we examined the effect of inhibition of LOX-1 on the ox-LDL-induced RhoA and Rac1 activation. Pretreatment of HAECs with TS92 (10 μg/mL) for an hour prevented ox-LDL-induced RhoA and Rac1 activation 5 and 15 min after exposure to ox-LDL, respectively (*Figure 1C* and *D*). This indicated an integral role of LOX-1 in ox-LDL-induced RhoA and Rac1 activation.

3.2 Effect of TIMPs on RhoA and Rac1 activation induced by ox-LDL

To clarify the relation between secreted MMPs or MT-MMPs and LOX-1-mediated RhoA and Rac1 activation, HAECs were pretreated with 40 nmol/L TIMP-1 and TIMP-2 for 60 min before adding ox-LDL. *Figure 2A* and *B* show that TIMP-2, but not TIMP-1, inhibited the GTP-loading of RhoA and Rac1 caused by ox-LDL. TIMP-1 or TIMP-2 alone did not alter the basal levels of RhoA and Rac1 in untreated HAECs (data not shown). These findings suggest that MT-MMPs are upstream of ox-LDL-triggered RhoA and Rac1 activation.

3.3 MT1-MMP activity

Since MT1-MMP is one of the well-characterized MT-MMPs, we first measured the activity of MT1-MMP in response to ox-LDL stimulation within 30 min. Ox-LDL induced a significant increase in the activity of MT1-MMP after 15 and 30 min of stimulation (*Figure 3*).

3.4 Role of MT1-MMP in ox-LDL-induced RhoA and Rac1 signalling

Then, we examined the role of MT1-MMP in ox-LDL-induced RhoA and Rac1 activation through LOX-1. HAECs were transfected with siRNA to MT1-MMP before exposure to ox-LDL. In the transfected cells, knockdown of MT1-MMP prevented the ox-LDL-triggered activation of RhoA and Rac1 as determined by pull-down assays (*Figure 4A* and *B*). *Figure 4C* shows the effect of the transfection of MT1-MMP siRNA on the MT1-MMP protein level as determined by western blotting, indicating the approximately 70% reduction in the MT1-MMP level by treatment with the siRNA.

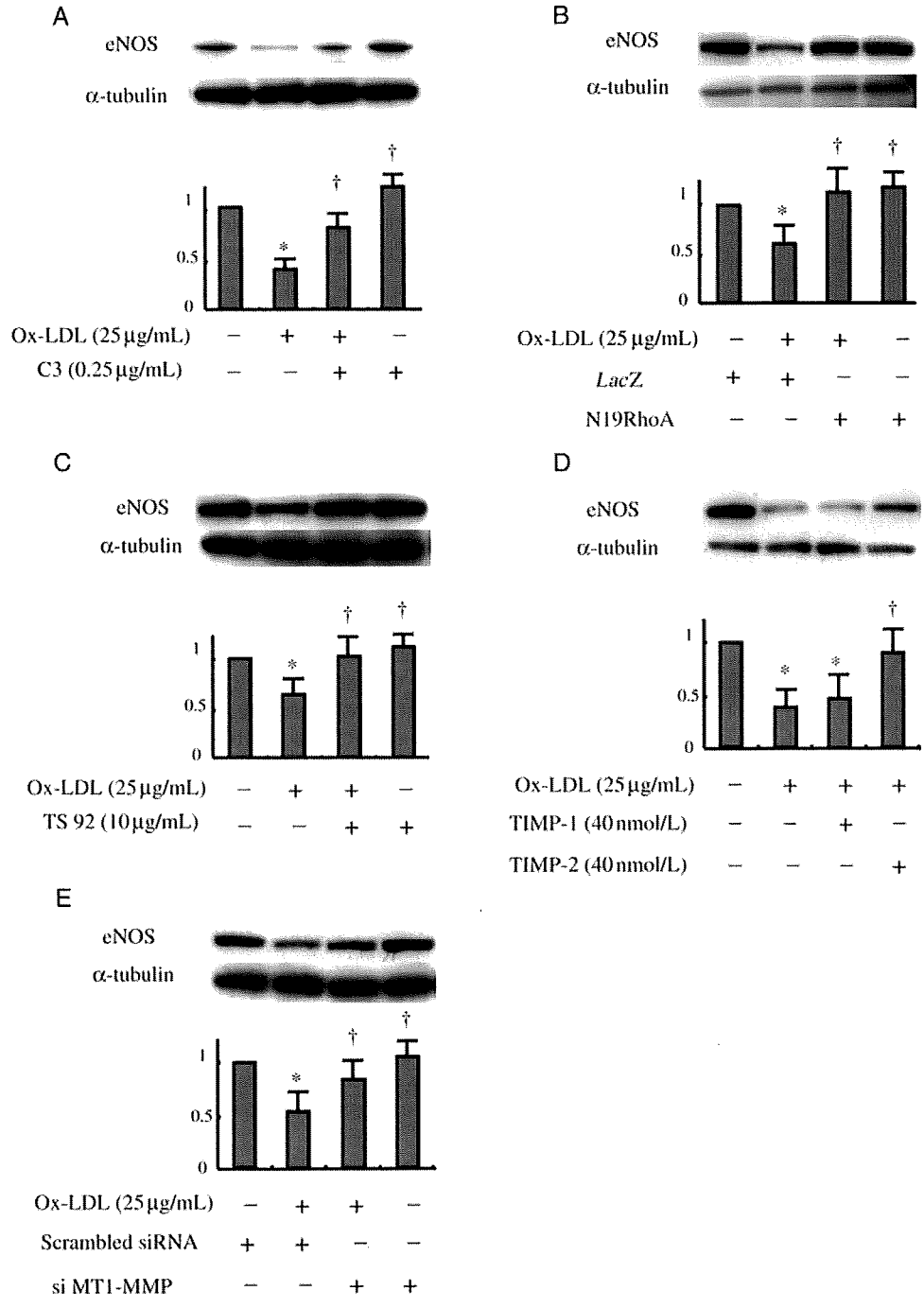

Figure 6 Role of the LOX-1/MT1-MMP axis in RhoA-dependent eNOS protein expression. (*A*, *B*) Effect of inhibition of RhoA by C3 exoenzyme and N19RhoA on ox-LDL-induced eNOS downregulation. HAECs were treated with 0.25 μg/mL of C3 exoenzyme overnight or infected with adenoviruses encoding N19RhoA or *LacZ* and then stimulated with 25 μg/mL ox-LDL for 18 h, followed by western blotting. (*C*) Effect of inhibition of LOX-1 on ox-LDL-induced eNOS downregulation. Cells were treated with 10 μg/mL TS92 for 1 h and then stimulated with 25 μg/mL ox-LDL for 18 h, followed by western blotting. (*D*, *E*) Effects of TIMP-2 and knockdown of MT1-MMP on ox-LDL-induced eNOS downregulation. Immunoblots are from an experiment representative of four similar experiments. Quantitative results of eNOS expression were normalized by α-tubulin levels. Bars are mean ± SD of quantitative densitometric analyses from three separate experiments. $^{*}P < 0.05$ vs. control; $^{\dagger}P < 0.05$ vs. ox-LDL.

3.5 Molecular interaction of LOX-1 and MT1-MMP

To determine the distribution of LOX-1 and MT1-MMP in cultured HAECs, we performed immunostaining. *Figure 5A* shows the expression of LOX-1 and MT1-MMP, as well as the merged image, respectively, indicating that LOX-1 was partially colocalized with MT1-MMP in HAECs.

To clarify the interaction of LOX-1 with MT1-MMP, we first performed the immunoprecipitation using an initial antibody to LOX-1. Although little or no expression was detected by normal mouse IgG as a negative control antibody (*Figure 5B*, left panel, lane 1), the band of 64 kDa of MT1-MMP was detected in the LOX-1-associated immunoprecipitates (*Figure 5B*, left panel, lane 2). Counter experiment using anti-MT1-MMP antibody revealed that the band of LOX-1 (Mr 70 kDa) was recognized in the MT1-MMP-immunoprecipitates (*Figure 5B*, right panel, lane 2). These

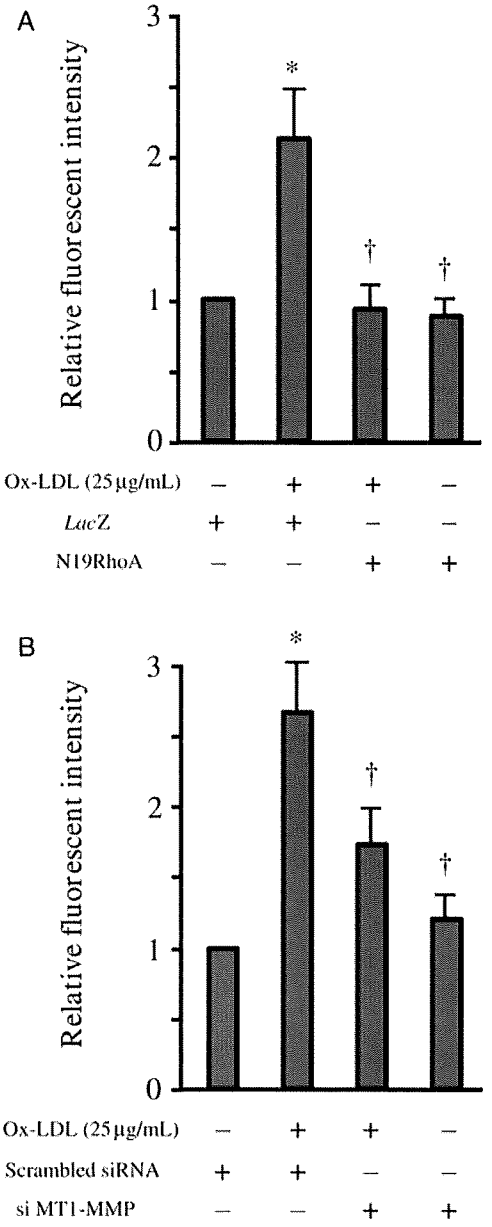

Figure 7 Role of the MT1-MMP/RhoA axis in endothelial cell invasion. HAECs were treated with N19RhoA (*A*) or MT1-MMP siRNA (*B*) and then stimulated with 25 μg/mL ox-LDL for 4 h, followed by cell invasion assays. Data are expressed as mean ± SD of an experiment representative of four separate experiments. *$P < 0.01$ vs. control; †$P < 0.01$ vs. ox-LDL.

results strongly suggested that LOX-1 forms a complex with MT1-MMP. Exposure to ox-LDL did not change the level of formation of LOX-1 and MT1-MMP (data not shown).

3.6 Role of MT1-MMP-RhoA axis in ox-LDL-induced downregulation of eNOS protein expression

First, we confirmed that ox-LDL-induced downregulation of eNOS protein expression is mediated via RhoA activation in our culture system. Inhibition of RhoA by C3 exoenzyme (*Figure 6A*) and dominant-negative RhoA (*Figure 6B*) reversed ox-LDL-induced decrease of eNOS protein expression. Treatment of HAECs with TS92 for LOX-1 inhibition reversed the ox-LDL-induced eNOS protein downregulation after 18 h of incubation (*Figure 6C*). In addition, TIMP-2, but not TIMP-1, prevented ox-LDL-induced downregulation of eNOS protein expression (*Figure 6D*). Ox-LDL-induced eNOS protein downregulation was also reversed in the MT1-MMP-silenced cells, whereas scrambled siRNA had no effect (*Figure 6E*).

3.7 Role of RhoA-MT1-MMP axis in cell invasion

To further clarify the role of the MT1-MMP/RhoA axis in RhoA-mediated events, we performed an endothelial invasion assay. Ox-LDL-induced EC invasion was attenuated by N19RhoA, indicating the RhoA-dependent mechanism (*Figure 7A*). Pretreatment of HAECs with silencing of MT1-MMP by siRNA suppressed the oxidized LDL-triggered EC invasion (*Figure 7B*).

3.8 Role of LOX-1-MT1-MMP axis in NADPH oxidase-dependent ROS generation

The levels of intracellular ROS generation were increased 1 h after exposure to ox-LDL (*Figure 8A* and *B*), which was prevented by TS92 (*Figure 8A* and *C*) as well as by DPI and N17Rac (*Figure 8A*, *E*, and *I*). These indicated that ox-LDL-induced ROS generation occurs via Rac1/NADPH oxidase through LOX-1. Silencing of MT1-MMP by siRNA significantly blocked ox-LDL-triggered ROS generation and NADPH oxidase activity (*Figures 8B* and *C*).

4. Discussion

In this study we demonstrated the crucial role of MT1-MMP in LOX-1-initiated RhoA- and Rac1-dependent signalling pathways in ox-LDL stimulation in ECs. Another important finding of the present study is that LOX-1 forms a complex with MT1-MMP. Here, we propose the concept of the regulation of ox-LDL-induced endothelial dysfunction by the LOX-1-MT1-MMP axis.

For the first time we show that knockdown of MT1-MMP markedly attenuated rapid RhoA and Rac1 activation caused by ox-LDL via LOX-1. Meriane *et al.*[27] have shown that GM6001, a broad spectrum of MMP inhibitor, blocked sphingosine-1-phosphate-induced RhoA activation within 1 min in bone marrow-derived stromal cells, suggesting cooperation between MMP-mediated signalling events and RhoA signalling pathway. Our experiments demonstrated that GM6001 (data not shown) and TIMP-2, but not TIMP-1, prevented ox-LDL-triggered rapid RhoA and Rac1 activation in HAECs, suggesting that extracellular domain of MT1-MMP may play a role in the signal transduction of ox-LDL-exposed cells via LOX-1. In fact, the increase in MT1-MMP activity was induced by ox-LDL within 15 min. However, the detailed mechanism(s) remain(s) to be clarified.

The present study indicates that MT1-MMP is upstream of ox-LDL-stimulated RhoA and Rac1 activation. It is generally accepted that MT1-MMP is an MMP-2 activator.[13,28,29] This raises the issue whether or not inhibition of MMP-2 might prevent ox-LDL-triggered RhoA and Rac1 activation in our experimental system. We found that TIMP-1, which inhibits MMP-2 but not MT-MMPs, did not suppress the ox-LDL-dependent RhoA and Rac1 activation. These results suggest that MMP-2 is not involved in ox-LDL-triggered RhoA and Rac1 signalling pathways in ECs.